Int J Earth Sci (Geol Rundsch) (2018) 107:885–911
https://doi.org/10.1007/s00531-017-1520-7

ORIGINAL PAPER

# A ~565 Ma old glaciation in the Ediacaran of peri-Gondwanan West Africa

**Ulf Linnemann[1] · Agustín Pieren Pidal[2] · Mandy Hofmann[1] · Kerstin Drost[3] · Cecilio Quesada[4] · Axel Gerdes[5] · Linda Marko[5] · Andreas Gärtner[1] · Johannes Zieger[1] · Jens Ulrich[6] · Rita Krause[1] · Patricia Vickers-Rich[7,8,9,10] · Jana Horak[11]**

Received: 28 February 2017 / Accepted: 16 July 2017 / Published online: 16 August 2017


**Abstract** In the Cadomian orogen of the NE Bohemian Massif and of SW Iberia, a post-Gaskiers glacial event dated at c. 565 Ma has been detected. Such Ediacaran-aged glaciomarine deposits occur in the Weesenstein and Clanzschwitz groups of the Saxo-Thuringian zone (Bohemia) and in the Lower Alcudian group of the southern Central Iberian zone (Iberia). Both areas are parts of Cadomia situated in the Western and Central European Variscides. Glaciomarine sedimentary rocks are characterized by such features as dropstones, flat iron-shaped pebbles ("*Bügeleisen-Geschiebe*"), facetted pebbles, dreikanters, and zircon grains affected by ice abrasion. For age and provenance determination, LA–ICP–MS U–Pb ages ($n = 1124$) and Hf isotope ($n = 446$) analyses were performed. The maximum age of the glaciomarine deposits within a Cadomian back-arc basin based on U–Pb analytics resulted in the youngest detrital zircon populations showing ages of 562–565 Ma and of c. 566–576 Ma old zircon derived from granitoid pebbles within the diamictites. The youngest age recorded was 538–540 Ma based on zircon from the plutons which had intruded the previously deformed Ediacaran metasedimentary rocks. Previously described glaciomarine diamictites of Cadomia (Weesenstein, Clanzschwitz, and Orellana diamictites) are most definitely younger than the

**Electronic supplementary material** The online version of this article (doi:10.1007/s00531-017-1520-7) contains supplementary material, which is available to authorized users.

✉ Ulf Linnemann
ulf.linnemann@senckenberg.de

Agustín Pieren Pidal
apieren@geo.ucm.es

Mandy Hofmann
mandy.hofmann@senckenberg.de

Kerstin Drost
drostk@tcd.ie

Cecilio Quesada
quesada.cecilio@gmail.com; cquesada@ucm.es

Axel Gerdes
gerdes@em.uni-frankfurt.de

Linda Marko
marko@em.uni-frankfurt.de

Andreas Gärtner
andreas.gaertner@senckenberg.de

Johannes Zieger
johannes.zieger@senckenberg.de

Jens Ulrich
jens.ulrich@gub-ing.de

Rita Krause
rita.krause@senckenberg.de

Patricia Vickers-Rich
pat.rich@monash.edu; prich@swin.edu.au

Jana Horak
jana.horak@museumwales.ac.uk

[1] Senckenberg Naturhistorische Sammlungen Dresden, Museum für Mineralogie und Geologie, GeoPlasmaLab, Königsbücker Landstraße 159, 01109 Dresden, Germany

[2] Departmento de Estratigrafía, Universidad Complutense, 28040 Madrid, Spain

[3] Department of Geology, School of Natural Sciences, Trinity College Dublin, Dublin 2, Ireland

[4] Instituto Geológico y Minero de España, Ríos Rosas 23, 28003 Madrid, Spain

[5] Institut für Geowissenschaften, Mineralogie, Goethe-Universität Frankfurt, Altenhöferallee 1, 60438 Frankfurt am Main, Germany

[6] G.U.B. Ingenieur AG, Niederlassung Freiberg, Halsbrücker Straße 34, 09599 Freiberg, Germany

c. 579–581 Ma Gaskiers glaciation in Newfoundland (Gaskiers) and in SE New England (Squantum). We propose the term *Weesenstein–Orellana glaciation* for this new Ediacaran glacial event, named after the most relevant regions of exposure. Palaeogeographically, these glaciomarine diamictites and related sedimentary deposits lie on the periphery of the West African Craton (western peri-Gondwana), and evidence has been provided by detrital zircon U–Pb ages and their Hf isotope composition. Correlation with similar glaciomarine deposits in the Anti-Atlas (Bou Azzer) and Saudi Arabia suggests a continued distribution of post-Gaskiers glacial deposits along the Gondwana margin of Northern Africa. The *Weesenstein–Orellana glaciation* correlates in part with the Shuram–Wonoka $\delta^{13}C$ anomaly.

**Keywords** Glaciation · Ediacaran · Weesenstein–Orellana glaciation · Neoproterozoic palaeoclimate · peri-Gondwana · West African craton · Cadomian orogeny · U–Pb zircon ages · Hf isotopes

## Introduction

Glaciations have a major impact on the evolution of life and affect the entire planet Earth (Hoffman 2009). Neoproterozoic glaciations played a major role as a bottleneck, and upon melting a major driver, for the origin of first large multicellular life, and the rise of the Ediacaran biota (Narbonne and Gehling 2003; Vickers-Rich and Fedonkin 2007). Cryogenian (c. 850–635 Ma) strata record the most extreme climate episodes in Earth's history. The widespread occurrence of low-latitude glacial deposits globally together with the unusual geochemistry and sedimentology of cap carbonates (Hoffman et al. 1998; Bao et al. 2008) inspired the hypothesis of Snowball Earth (Kirschvink 1992, Kirschvink et al. 2000). Timing of Cryogenian glaciations is well established, represented by the Marinoan and Sturtian Snowball Earth events. The Marinoan Snowball Earth (Hoffman et al. 1998) is bracketed between c. 635 and 639 Ma (Hoffmann et al. 2004; Prave et al. 2016). Its predecessor, the Sturtian snowball, began around 717 Ma and ended at c. 660 Ma (Macdonald et al. 2010; Rooney et al. 2015). Cryogenian global glacial events were followed by a mid-Ediacaran Gaskiers glaciation aged between c. 581 and 579 Ma (Pu et al. 2016). The global nature of the Gaskiers ice age is still under debate. It is noteworthy that elements of the Ediacaran biota are first recorded about 5 Ma after the Gaskiers glaciomarine deposition of the Drook Formation, exposed on the Avalon Peninsula (Newfoundland) and hosting the Avalon assemblage, the oldest known community of large multicellular organisms on Earth (Narbonne et al. 2012, 2014).

Here, we introduce a new post-Gaskiers glacial event recorded in upper Ediacaran-aged strata occurring in the Cadomian orogen of Gondwanan Europe (Fig. 1). We present evidence for glaciomarine sedimentation in late Neoproterozoic evidenced in strata from the Saxo-Thuringian zone of the Central European Variscides (Germany) and from the Central Iberian zone of the Variscides in Spain. These sedimentary units are characterized by glaciomarine sedimentary features. Their maximum age is provided by U–Pb dates of youngest detrital zircon populations and of magmatic zircon from granitoid pebbles within the diamictites. U–Pb ages and Hf isotopes of detrital zircon were used as provenance indicators. We integrate all new data with the previous records and proposed the existence of a new late Ediacaran glacial episode.

## Geological setting

The Cadomian orogeny culminating at the end of the Precambrian and the earliest Cambrian is the principal pre-Variscan orogenic event in both the Bohemian Massif and Iberia (Fig. 1). Cadomian orogenic processes are characterized by a wide range of geotectonic events that took place in a marginal setting at the periphery of NW and N Africa from c. 750 to 540 Ma (e.g., Linnemann et al. 2000, 2014; Gutiérrez-Alonso et al. 2003; Drost et al. 2011). The type area for the Cadomian orogeny is the Armorican massif in north-western France (e.g., Graindor 1957). Rocks related to the Cadomian orogeny are commonly referred to by the collective term "Cadomian basement".

### Glacial deposits in the Saxo-Thuringian zone (Bohemian massif)

Our study focuses on rocks from the passive margin of the Cadomian arc–back-arc system (Linnemann 2007; Linnemann et al. 2014), best preserved in the Elbe zone and the North Saxon antiform in the southeastern part of the Saxo-Thuringian zone (NE Bohemian massif) (Fig. 2). In particular, we investigated the Ediacaran-aged Weesenstein and Clanzschwitz groups (Linnemann 2007). Furthermore, we included in our research the granodiorites of Laas and

[7] Department of Chemistry and Biotechnology, Faculty of Science, Swinburne University of Technology, Melbourne (Hawthorn), VIC 3122, Australia

[8] School of Earth, Atmosphere and Environment, Monash University, Melbourne (Clayton), VIC 3800, Australia

[9] School of Environmental Sciences, Deakin University, Melbourne (Burwood), VIC, Australia

[10] Palaeontology Department, Museum Victoria, Carlton Gardens, Melbourne, VIC 3001, Australia

[11] National Museum Cardiff, Mineralogy and Petrology, Cathays Park, Cardiff CF10 3NP, UK

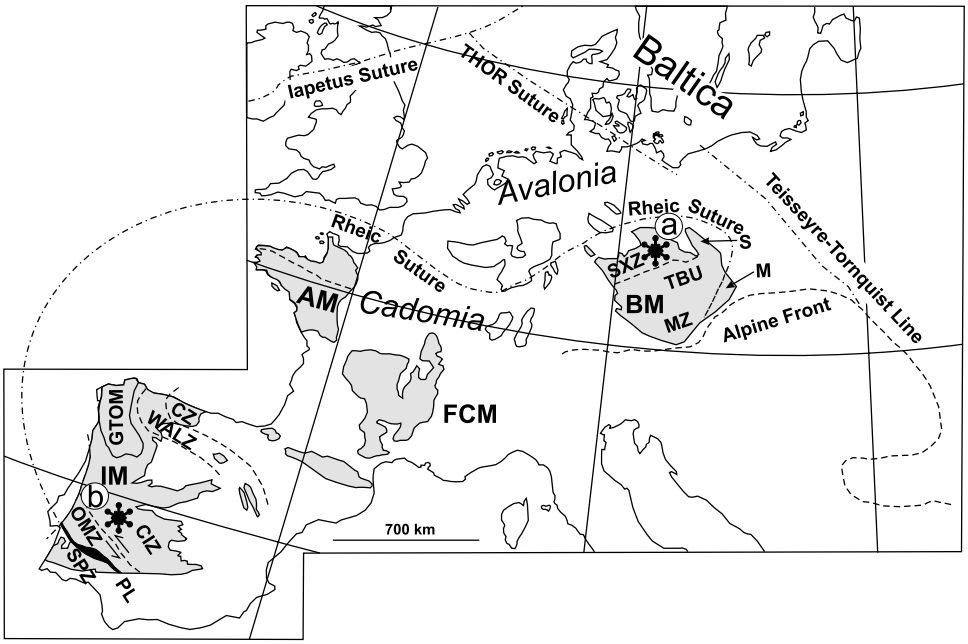


**Fig. 1** Location of Variscan massifs in Central and Western Europe. *AM* Armorican massif, *BM* Bohemian massif, *FCM* French Central massif, *IM* Iberian massif, *M* Moravo-Silesian unit, *S* Sudetes. Variscan zones: *CIZ* Central Iberian, *CZ* Cantabrian, *GTOM* Galicia-Tras os Montes, *MZ* Moldanubian, *OMZ* Ossa-Morena, *PL* Pulo do Lobo, *SPZ* South Portuguese, *SXZ* Saxo-Thuringian, *TBU* Teplá-Barrandian unit, *WALZ* West asturian–Leonese. Ediacaran glaciomarine deposits in the Cadomian orogen: *a* Weesenstein and Clanzschwitz, *b* Orellana

Dohna (earliest Cambrian). These plutonic rocks intruded the Ediacaran sedimentary units at c. 540 Ma after their deformation (Linnemann et al. 2010a).

The Weesenstein group is exposed in the Elbe zone, which forms an NW–SE trending Variscan shear zone exhibiting a strong dextral strike-slip movement of at least 80–120 km sub-horizontal displacement (Linnemann 1994). Strike-slip movements took place in a time interval from c. 335 to 327 Ma (Hofmann et al. 2009). The Elbe zone divides the Variscan nappe pile of the Erzgebirge in the SW from the Lausitz Block in the NE (Fig. 2). While the latter consists mainly of Cadomian basement rocks (Lausitz Greywacke complex, and Lausitz Granodiorite complex, Linnemann et al. 2010a), the Erzgebirge is composed of a complex Variscan nappe pile of at least four separate nappes characterized by low pressure, and high and ultra-high pressure rocks (e.g. Sebastian 2013 and references therein). After reaching crustal levels at c. 340 Ma, and exhumation a short time later, a top-to-NW directed final emplacement was responsible for the origin of the dextral strike-slip movements along the Elbe zone (Linnemann 1994; Linnemann et al. 2010b and references therein). The Elbe zone is fault-bounded against the Erzgebirge nappe pile by the Mid Saxon fault, whereas the northern limit is the northern branch of the West Lausitz fault (Fig. 2). Variscan basement rocks of the Elbe zone show a protolith age range from the Ordovician to the Early Carboniferous and crop out in the Elbtalschiefergebirge (SE of Dresden) as well as in the Nossen-Wilsdruff Schiefergebirge (Fig. 2). Cadomian basement rocks form a narrow strip on the northeastern flank of the Elbe zone. In the Elbtalschiefergebirge (Figs. 2, 3), outcrops of the Weesenstein group and the Dohna granodiorite occur. Here, the Weesenstein group (Figs. 2, 3) is fault-bounded against Palaeozoic rocks along its southwestern limit by the southern branch of the West Lausitz fault. The strip of Cadomian rock units continues towards the northwest and is represented north of the Meißen massif by the Rödern group and the Großenhain orthogneiss (Fig. 2). The Cadomian basement of the Elbe zone continues further to the northwest into the North Saxon antiform. In that area, the Cadomian basement units of the Clanzschwitz group and the Laas granodiorite are present (Fig. 2). The complex pluton of the Meissen massif intruded into the strike-slip regime of the Elbe zone at 334 ± 3 Ma (Hofmann et al. 2009), emplaced into the southern branch of the West Lausitz fault, a distinct zone of weakness at that time (Linnemann 1994). Variscan strike-slip movements had ceased by 327 ± 3 Ma, the timing of intrusion of the Markersbach granite (Hofmann et al. 2009) that crosscuts all faults and cleavage planes in country rocks and thus provides a perfect time marker for the cessation of the Variscan strike-slip movement and the end of Variscan deformation in the region (Hofmann et al. 2009). At the beginning of the Permian, subsidence and felsic volcanism began in the Elbe zone resulting in formation of the Döhlen basin during the Rotliegend (Fig. 2) (Hofmann et al. 2009; Zieger 2015). This is the region in which the Weesenstein group and Dohna granodiorite outcrop were mapped in detail by Linnemann (1990, 1991). In the c. 2500 m-thick Weesenstein group, the older Seidewitz formation (c. 1500 m) occurs in the SW, while the younger Müglitz formation (c. 1000 m) is located in the NE. The section is rootless and fault-bounded at the base of the Seidewitz formation by the southern branch of the Westlausitz fault (Fig. 4). The Müglitz formation is limited by the intrusive contact with the Dohna granodiorite

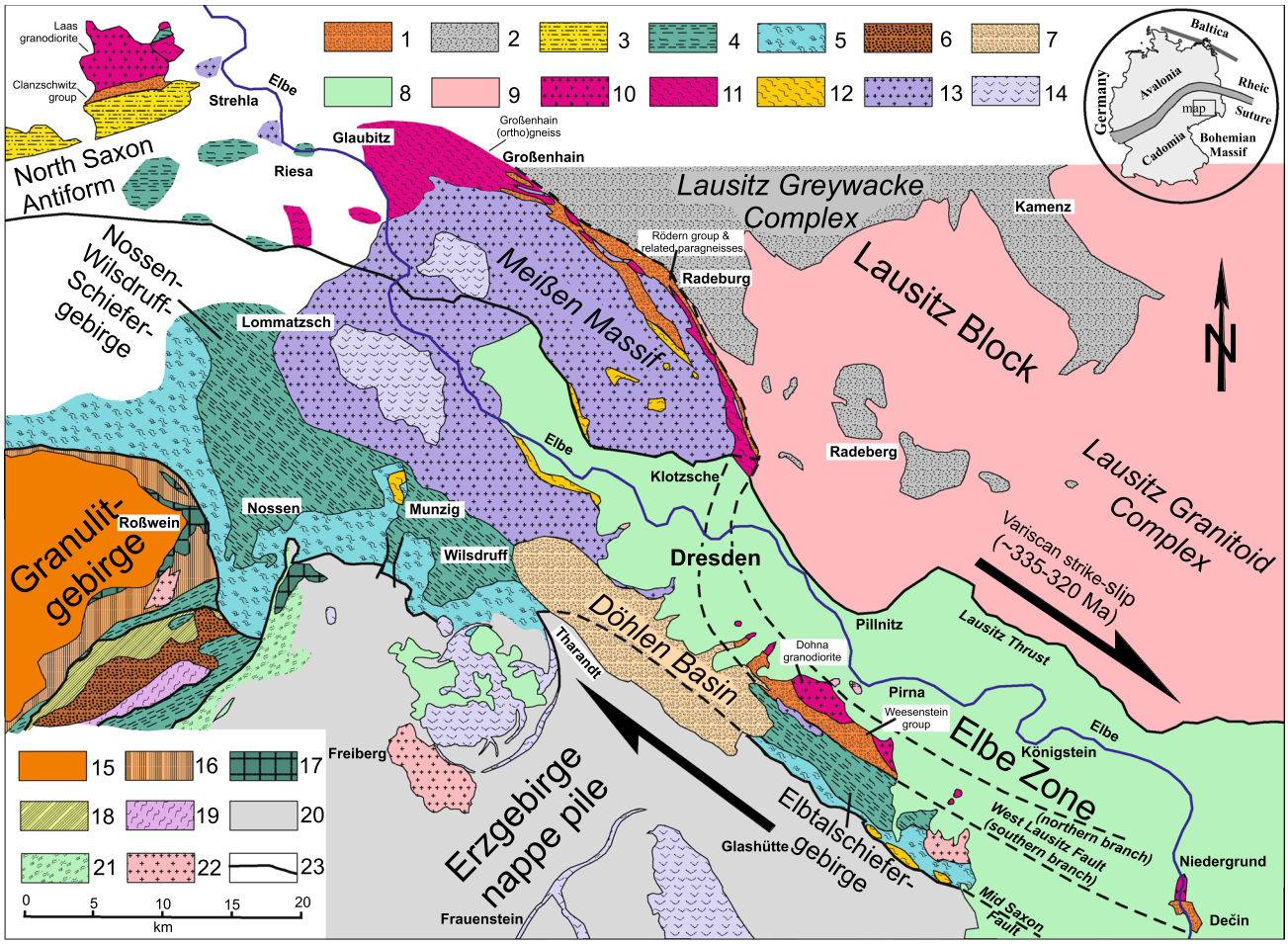


**Fig. 2** Geological map of the Elbe zone and adjoining geological units showing the position of the Weesenstein, Clanzschwitz, and Rödern groups (Ediacaran) (modified from Pietzsch 1927; Linnemann 2007). *1* diamictites, quartzites, greywackes, and other siliciclastic metasedimentary rocks of the Weesenstein, Clanzschwitz, and Rödern groups (Ediacaran), *2* greywackes and mudstones (Ediacaran, Lausitz Greywacke complex), *3* Cambro-Ordovician quartzites and quartz schists, *4* Palaeozoic rocks not subdivided (Ordovician to Early Carboniferous), *5* Phyllitic Unit of the Elbe zone (Mühlbach-Nossen group, Cambro-Ordovician, to Devonian protoliths), *6* Early Variscan molasses of Hainichen (upper Viséan), *7* Rotliegend (Early Permian Variscan molasses), *8* Late Cretaceous, *9* granodiorites and anatexites (c. 540 Ma, Lausitz Granitoid complex), *10* Granodiorites of Dohna and Laas (c. 540 Ma, Elbe zone), *12* Großenhain orthogneiss, *13* Meißen massif (c. 335 Ma, not subdivided, monzonites, diorites, granites), *14* Upper Carboniferous volcanic and sub-volcanic rocks, *15* granulites of the Granulitgebirge ("Saxonian Granulites", Variscan metamorphic core complex), *16* schist belt on the periphery of the Granulitgebirge, *17* flasergabbro, *18* greenschists (prasinites), *19* orthogneiss (c. 490 Ma) of the Frankenberg Zwischengebirge (Variscan nappe complex), *20* gneisses and other lithologies of the Erzgebirge nappe pile (high- and ultra-high-pressure rocks, not subdivided), *21* phyllites and other lithologies of the Erzgebirge nappe pile (low pressure rocks, not subdivided), *22* Variscan granitoids (c. 335–320 Ma), *23* major fault

(Figs. 3, 4). The latter is dated at c. 538 Ma (Pb–Pb age, Gehmlich 2003). The general metamorphic overprint is characterized by a mid-to-high greenschist grade (in part biotite grade). Bedding is sub-vertical with two pronounced cleavages (Cadomian, Variscan, Linnemann 1990). The older Seidewitz formation represents a pre-glacial deposit, while the younger Müglitz formation contains glaciomarine sedimentary rocks (Fig. 5).

The Seidewitz formation is composed primarily of shelf deposits, such as quartz schist, quartzite, quartz wacke, greywacke, and mudstone (Fig. 5a–d). A prominent part of the sedimentary pile is the Purpurberg quartzite member (Fig. A), a sedimentary sequence of medium-to-thick-bedded quartzites ("Purpurberg quartzite", Figs. 4, 5a, b) with quartz schist intercalations in the middle and conglomerate at the top (Fig. 5d). Primary sedimentary features, such as cross bedding and ripple marks (Fig. 5b), indicate that the lower part of the section is distributed in the SW, while the younger top in a transition to the overlying Müglitz formation occurs towards the NE (Fig. 4). The Purpurberg quartzite member represents the marine part of a fan delta deposit, which pinches out along strike towards the SE and to the

NW (Fig. 4) (Linnemann 2007). The depositional centre is located at the Purpurberg and the Hallstein regions (Fig. 5a) along both flanks of the valley of the Bahra River (Fig. 4) (Linnemann 1990). The Purpurberg member is thin-bedded in the more distal parts of the fan delta and perfectly visible in the outcrops of the "Röhrsdorfer Park" (Figs. 4, 5c). The Seidewitz formation is limited in completeness at the base by the tectonic contact of the southern branch of the West Lausitz fault (Fig. 4). In that part of the formation, the geological situation becomes further complicated by intrusion of a Variscan hornblende granodiorite (Fig. 4), which is part of the Meissen massif (c. 335 Ma; Hofmann et al. 2009). Due to the contact-metamorphic overprint, most of the older part of the Seidewitz formation has been altered into an andalusite hornfels (Pietzsch 1917; Linnemann 1990). In its northwesternmost part, the Seidewitz formation was affected by partial melting and magmatization due to a contact-metamorphic overprint by the emplacement of the Meissen massif and strong shearing during the dextral strike-slip movements along the Elbe zone (Fig. 2) (Linnemann 1990). Within the Seidewitz formation, a number of amphibolites and meta-basalts occur (Fig. 4). In addition, one very badly exposed chert layer is known only from loose blocks found close to "Röhrsdorfer Park" (Pietzsch 1917) (Fig. 4).

The transition of the Seidewitz formation into the overlying (younger) Müglitz formation is gradual. The transitional interval is best exposed on the eastern flank of the Müglitz valley (Fig. 4) in the area northeast of the Weesenstein castle. Quartzite and quartz schist grade into greywacke, mudstone, and quartz wacke of the Müglitz formation. An additional, characteristic feature of the Weesenstein formation is occurrence of diamictites and conglomerates (Figs. 4, 5e–g). The diamictites crop out mainly along the flanks of the Müglitz Valley (Fig. 4). A few exposures are known in the valley of the Lockwitz River (Fig. 4) (Linnemann 1990). Isolated diamictite pebbles of granitoids, quartzite, and greywacke "swim" in a matrix of greywacke and mudstone (Fig. 5e, f), varying in size between 5 mm and 30 cm. Some of the pebbles are rounded and deformed due to Late Carboniferous tectonic overprint (Fig. 5e).

In some units, the diamictite is less deformed, particularly those cropping out around the railway station of Weesenstein. Here, diamictites which escaped penetrative deformation in the pressure shadows of more competent rock units, such as thick quartz wacke layers, can reach a thickness of more than 50 m. Glaciomarine features are documented by dropstones (Fig. 6a), dreikanters (Fig. 6b), flatiron-shaped pebbles ("*Bügeleisen-Geschiebe*") (Fig. 6c, d), and facetted pebbles (Fig. 6d, e). Typical rainout deposits, formed by melting icebergs, also occur (Fig. 6f), with randomly oriented and predominantly quartzite and greywacke pebbles (47.2%). The second-largest group represented is volcanic rocks, such as rhyolite, felsite porphyry (andesite), and keratophyre (22.7%). Only 15.0% are igneous in origin including granodiorite, aplitic granite, and granite. The remaining 15.1% of the pebbles are vein quartz and quartz derived from pegmatites (Schmidt 1960). The dominance of sedimentary rocks among the loose pebbles in the diamictite is an additional argument for its glaciomarine origin, because glaciers erode mainly the shelf deposits in the source area before became floating ice.

In addition to the observations of glaciomarine features in the macro-scale, we carried out studies on zircon surfaces recovered from the diamictites of the Müglitz formation and compared them with such surfaces derived from a sub-recent Quarternary lodgement till from Germany (Isle of Rügen, coastline north of Saßnitz, Fig. 7). Features indicative of glacial transport for detrital grains include high angularity, fresh faces, conchoidal breaks, and arc-step-like fractures reported by Immonen (2013). SEM backscatter images of investigated zircon grains show clear effects of ice abrasion in the Quarternary lodgement till (Fig. 7a–f), similar to such surfaces on the zircons recovered from the glaciomarine rainout deposit of the Weesenstein group (Fig. 7g–q, sample WST 1, Müglitz formation). Zircons from both samples exhibit scratches, flatiron shapes with relatively sharp top and stump end, and rip-up structures generated in the pressure shadows during ice abrasion. Edges of rip-ups had been sub-rounded subsequently during sedimentation processes and demonstrate that they are not formed during heavy mineral separation by the jaw crusher. Some zircon grains exhibit shortening by compression characterized by a release band running vertical to compressive strain (Fig. 7f, p). Cathodoluminescence images of zircons from the Weesenstein diamictite reflect a wide range of different tectonomagmatic settings from which such zircon grains were derived (Fig. 8). Most zircons show normal magmatic zoning, and this points to a felsic provenance. Complex zircons with core and rim are common. Other grains seem to have been derived from mafic melts or rocks which underwent ultra-high-pressure metamorphism.

Within the Elbe zone and the North Saxon antiform, rock units exist, which are related to the Weesenstein group. Towards the northeast, the Cadomian basement of the Elbe zone continues into the Radeburg area, bound by the northern and southern branches of the Westlausitz fault (Fig. 2). Here, Cadomian rocks are preserved in a narrow strip of meta-greywackes (Rödern group). Bedding and cleavage run sub-vertical. Locally layers of diamictite occur at Brotberg Mountain near Rödern (Schmidt 1960). The metasediments of the Rödern group exhibit a metamorphic overprint generated under greenschist facies conditions (biotite grade) and were intruded at c. 540 Ma by a protolith of the Großenhain orthogneiss (Fig. 4) (Schmidt 1960; Gehmlich 2003). During the Variscan strike-slip movements along the Elbe

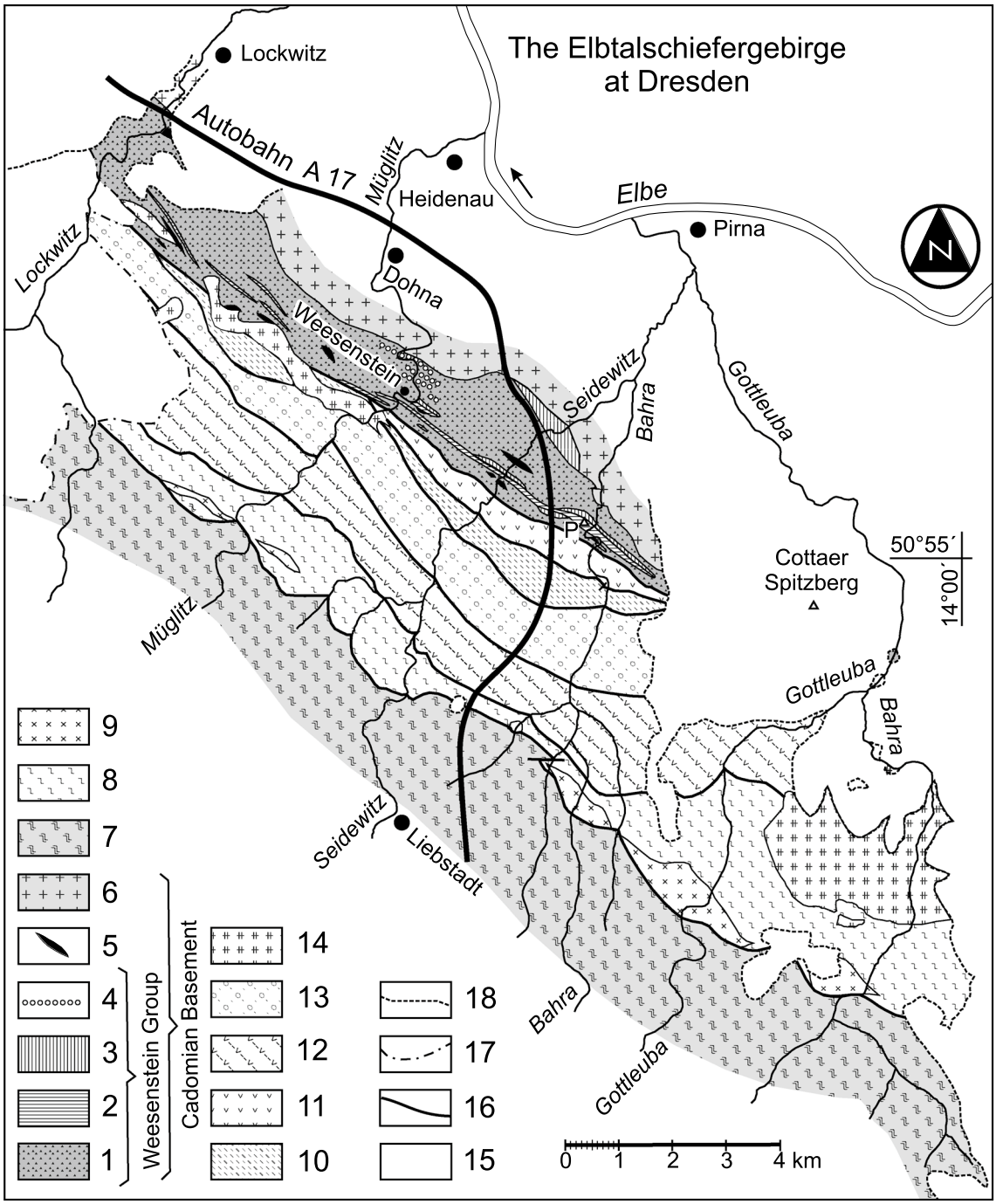


zone, the Cadomian basement strip was intruded by the c. 335 Ma old Meißen massif magma (Hofmann et al. 2009) (Fig. 2). The Rödern group is a strongly deformed equivalent of the Weesenstein group, while the Großenhain orthogneiss is a highgrade overprinted continuation of the Dohna granodiorite.

In the North Saxon antiform, about 30 km to the NW, there is a third area of importance with a Cadomian basement unit (Fig. 2). The metasedimentary Clanzschwitz group is subdivided into three un-named members (Fig. 9). The entire group is about 850 m thick and shows sub-vertical bedding and cleavage. Member 1 is composed of mudstones and quartz schists, and was intruded by the Laas granodiorite in the Early Cambrian. The strong contact metamorphism led to the origin of up to ~1 cm andalusite crystals. The second member of the Clanzschwitz group is composed of quartzite and quartz schist. Member 3 hosts diamictite (Clanzschwitz diamictite) and conglomerate layers (Fig. 5g). The Clanzschwitz group was intruded by the Laas granodiorite at c. 533 Ma (Pb–Pb age, Gehmlich 2003), and underwent

◂**Fig. 3** Geological map of the Elbtalschiefergebirge at Dresden (modified from Linnemann et al. 2008). *1* Weesenstein group containing the older Seidewitz formation including the Purpurberg Quartzite member and the younger Müglitz formation (Ediacaran), *2* Purpurberg quartzite member and its equivalents (Seidewitz formation, Weesenstein group, Ediacaran), *3* Quartz schists often under- and overlying the Purpurberg quartzite member (Seidewitz formation, Weesenstein group, Ediacaran), *4* Isolated pebbles and conglomerates of glaciomarine origin (Müglitz formation, Weesenstein group, Ediacaran), *5* Meta-basalts (Weesenstein group, Ediacaran), *6* Dohna granodiorite (Early Cambrian), *7* Cadomian metasediments of the Erzgebirge block overprinted under upper greenschist to amphibolite facies conditions during Variscan orogenic processes, *8* Ordovician, Silurian and Devonian metasediments and volcanic rocks of the Elbtalschiefergebirge overprinted under greenschist facies conditions during Variscan orogenic processes (so-called "Phyllitic unit" of the Elbe zone or Mühlbach-Nossen group), *9* Ordovician granite (Tourmaline granite, 485 ± 6 Ma, Linnemann et al. 2000), *10* Early Carboniferous metasediments, *11* Devonian volcano-sedimentary complex of the Elbtalschiefergebirge, *12* Devonian "diabase-limestone series" of the Elbtalschiefergebirge, *13* Early Carboniferous siliciclastic flysch deposits of the Elbtalschiefergebirge, *14* Variscan (Early Carboniferous) granitoids of the Meissen massif (c. 335 Ma) and the Markersbach granite (c. 320 Ma, Hofmann et al. 2009), *15* Permian and younger sedimentary cover, *16* major faults and dextral shear zones of the Elbtalschiefergebirge originated during Variscan orogenic processes, *17* Limit of Permian (Rotliegend) sedimentary rocks, *18* Limit of Cretaceous (Cenomanian–Turonian) sedimentary rocks, P-Top of the Purpurberg Mtn., type locality for the Purpurberg quartzite member

a high greenschist facies and biotite grade regional metamorphism. After a gap of sedimentation, the Cadomian basement in the North Saxon antiform was transgressed by Lower Ordovician sediments, preserved as quartzites and mudstones of the Collmberg formation (Pietzsch 1962), cropping out south of Clanzschwitz (Fig. 2).

The three described Cadomian basement exposures host the same geological unit which forms a ca. 60 km-long strip along the northeastern flank of the Elbe zone and at the southeastern margin of the North Saxon antiform (Fig. 2). The sedimentary and igneous parts of all three Cadomian basement units exhibit striking similarities. Both the older parts of the Clanzschwitz (members 1 and 2) and Weesenstein groups (Seidewitz formation, Purpurberg quartzite member) consist of quartzite and quartz schists. In the younger parts, both groups are composed of diamictites, greywackes, and conglomerates, also similar to the Müglitz formation (Weesenstein group) and member 3 of the Clanzschwitz group. In addition, the package of greywacke and mudstone in the Rödern group hosts diamictite horizons, poorly exposed at the Brotberg area near the village of Rödern (Schmidt 1960). The occurrence of facetted pebbles and the c. 60 km-wide distribution of diamictites in the Weesenstein, Clanzschwitz, and Rödern areas at the same lithostratigraphic level supports a glaciomarine nature of the diamictites (Linnemann 2007). All three sedimentary units of Cadomian basement in the Elbe zone were intruded by granodiorites of a similar age (c. 533–540 Ma, Pb–Pb ages by Gehmlich 2003). All in all, the Cadomian basement units of the Elbe zone share striking similarities. Thus, we assume that these units formed a single pre-Variscan rock unit along the southern margin of the Lausitz block. The formerly coherent unit of Cadomian passive margin sequences, including diamictite levels, was later sliced into the described three sub-units at Weesenstein, Rödern, and Clanzschwitz due to dextral strike-slip movements along the Elbe zone (Linnemann 1994; Linnemann et al. 2010a, b) in the c. 335–327 Ma time interval (Hofmann et al. 2009).

## Glacial deposits in the Central Iberian zone (Iberian massif)

Lotze (1945) proposed a division of the Iberian massif into six tectonostratigraphic zones, which still forms the basis of present subdivisions. Lotze's Eastern Lusitanian–Alcudian Zone is a 100–150 km-wide band that stretches from Coimbra–Castelo Branco–Cáceres to Ciudad Real and contains the glaciomarine diamictites dealt with herein. It was later merged with the Galician–Castillian Zone into the Central Iberian Zone by Julivert et al. (1972). Neoproterozoic rocks occur in most tectonostratigraphic domains of the Variscan orogen in Iberia interpreted to have once belonged to peri-Gondwanan Cadomia (Quesada 1990, 1991). The various divisions are thought to represent an arc/back-arc system (Ossa-Morena zone) accreted to a passive margin of West Africa on which a retro-arc basin developed (Central Iberian, West Asturian–Leonese, and Cantabrian zones) as a consequence of such arc accretion in late Neoproterozoic-earliest Cambrian time (Quesada 1990, 1991, 1996, 2006). Deformation associated with this arc-continent event characterizes the Cadomian orogeny in this part of peri-Gondwana and variably affected the various parts involved (Gutiérrez-Alonso et al. 2003). Among the different tectonostratigraphic zones in Iberia, the Central Iberian zone is by far the one of the largest and thickest exposures of Cadomian basement rocks (commonly known as Schist and Greywacke Complex in this area).

Ovtracht and Tamain (1970) studied the Proterozoic rocks of the Schist and Graywacke complex in the core of the Alcudia anticline. They subdivided the Ediacaran-aged sedimentary rocks into Lower and Upper Alcudian groups (Fig. 10) and subsequently integrated into the so-called Alcudian supergroup (San José et al. 1990) (Fig. 11). These rocks have also been called the Extremenian Dome group (Álvarez-Nava Oñate et al. 1988), a name which unfortunately has no relation to the investigated area. Therefore, the terms Lower and Upper Alcudian group are preferred here. In the area around Orellana, Ediacaran and lower Palaeozoic strata were mapped and studied in detail by Pieren (2000). The exposed Lower Alcudian group is about 4000 m

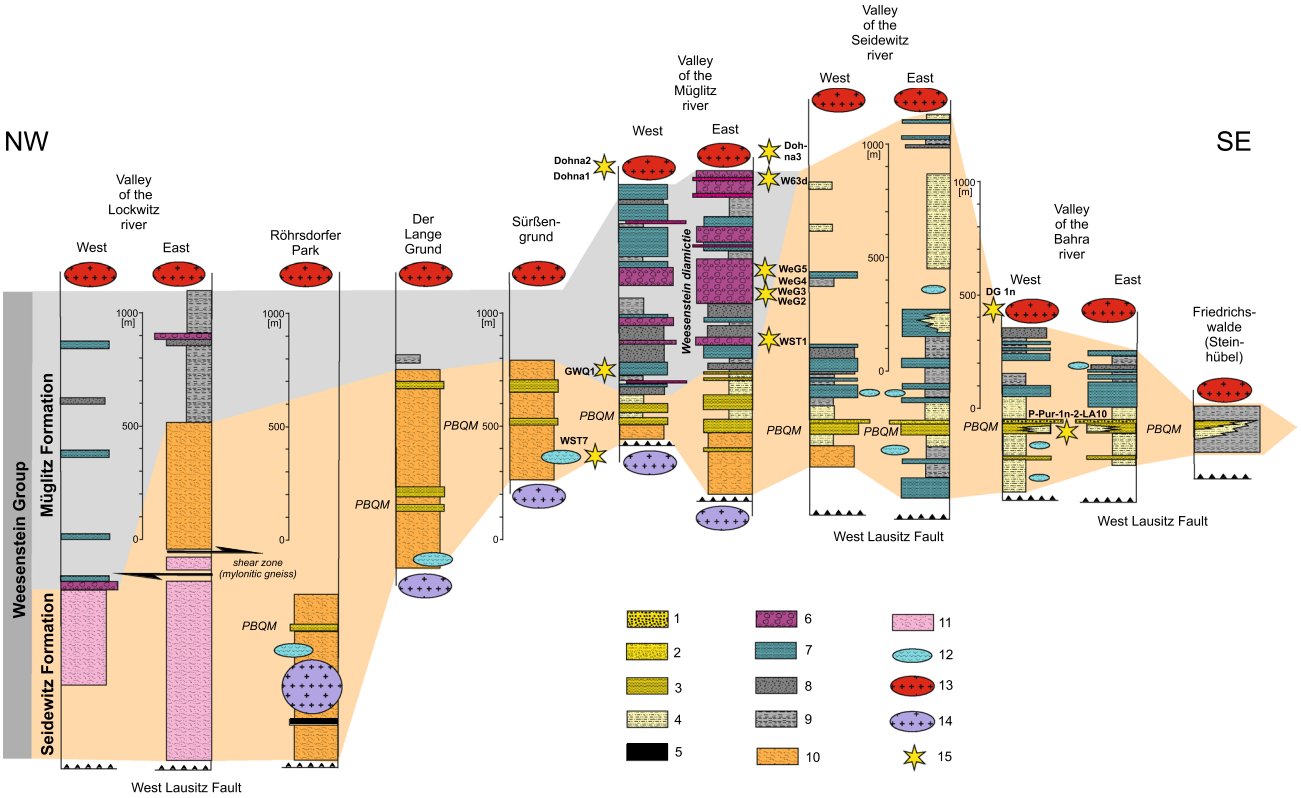


**Fig. 4** Lithostratigraphic columns of the Weesenstein group (Elbe zone, Elbtalschiefergebirge, Saxo-Thuringian zone) (from Linnemann 1990, 1991). *1* conglomerate with pebbles of quartz and hornfels (diameter of pebbles up to 3 cm); *2* conglomerate with pebbles of quartz and rarely hornfels (diameter of pebbles up to 1 cm); *3* quartzite of the Purpurberg quartzite member (PBQM) and related quartzite horizons of the Seidewitz formation; *4* quartz schist; *5* chert; *6* glaciomarine Weesenstein diamictite of the Müglitz formation ("Weesenstein tillite"); *7* quartz wacke (immature *greenish* quartzite); *8* greywacke; *9* mudstone; *10* andalusite quartzfels; *11* metasediments strongly sheared and overprinted by contact metamorphism, often partial anatectic melting initialized by contact metamorphism is indicated; *12* meta-basalts; *13* Dohna granodiorite (538 ± 2 Ma, this study); *14* Hornblende diorite of the Meißen massif (334 ± 3 Ma, Hofmann et al. 2009); *15* sample location; *PBQM* Purpurberg quartzite member

thick, but its base is nowhere exposed (Fig. 11). The group is characterized by a monotonous succession of turbidites composed of greywacke and mudstones (Fig. 11). According to García-Hidalgo et al. (1993) and Pieren (2000), the Lower Alcudian group from bottom to top is composed of (1) shales and greywackes ("La Coronada Shales formation"), (2) greywacke, microconglomerate, and shale ("Saint Mary of Zújar chapel greywackes and conglomerates formation"), and (3) shale, diamictite (pebbly mudstones), and greywacke ("Orellana matrix supported conglomerates formation") (Fig. 11). Some greywacke turbidite beds are up to 6 m thick and have been used as marker horizons during geological mapping of the region. Fuenlabrada et al. (2016) analyzed major and trace elements, REE, and Sm–Nd isotopes of greywacke samples of the second unit. Their geochemical results point to an active margin setting as the most reasonable source for the deposition of the Ediacaran–Early Cambrian sequences of the Central Iberian zone. Trace element diagrams of the Ediacaran greywackes indicate a clear affinity to a continental island arc which matches with the paleogeographic/paleotectonic interpretations mentioned above (Quesada 1991, 1996, 2006; Pieren 2000).

The Lower Alcudian group was folded and locally cleaved during the Cadomian orogenic activity. Generally, a vertical and sub-vertical $L_1$ lineation is present, which was generated by a (in the area) non-schistose gentle folding in the late Ediacaran ("intra-Alcudian" or Cadomian deformation). In addition, a Variscan schistose $F_1$ exists. Most cobbles were oriented parallel to a 70°N dipping $L_1$ lineation. Some of them were not oriented or almost normal to the $L_1$ lineation.

The Lower Alcudian group is unconformably overlain by the Upper Alcudian group (Fig. 11; Pieren 2000). This lithostratigraphic unit begins with conglomerates and coarse sandstones followed upsection by fine-grained sandstones and mudstones. Further upsection, shale and dolomite layers occur (Fig. 11). The basal unit of the Upper Alcudian group is considered to be latest Ediacaran. However, based on contained ichnofossils (Pieren 2000) and detrital zircons

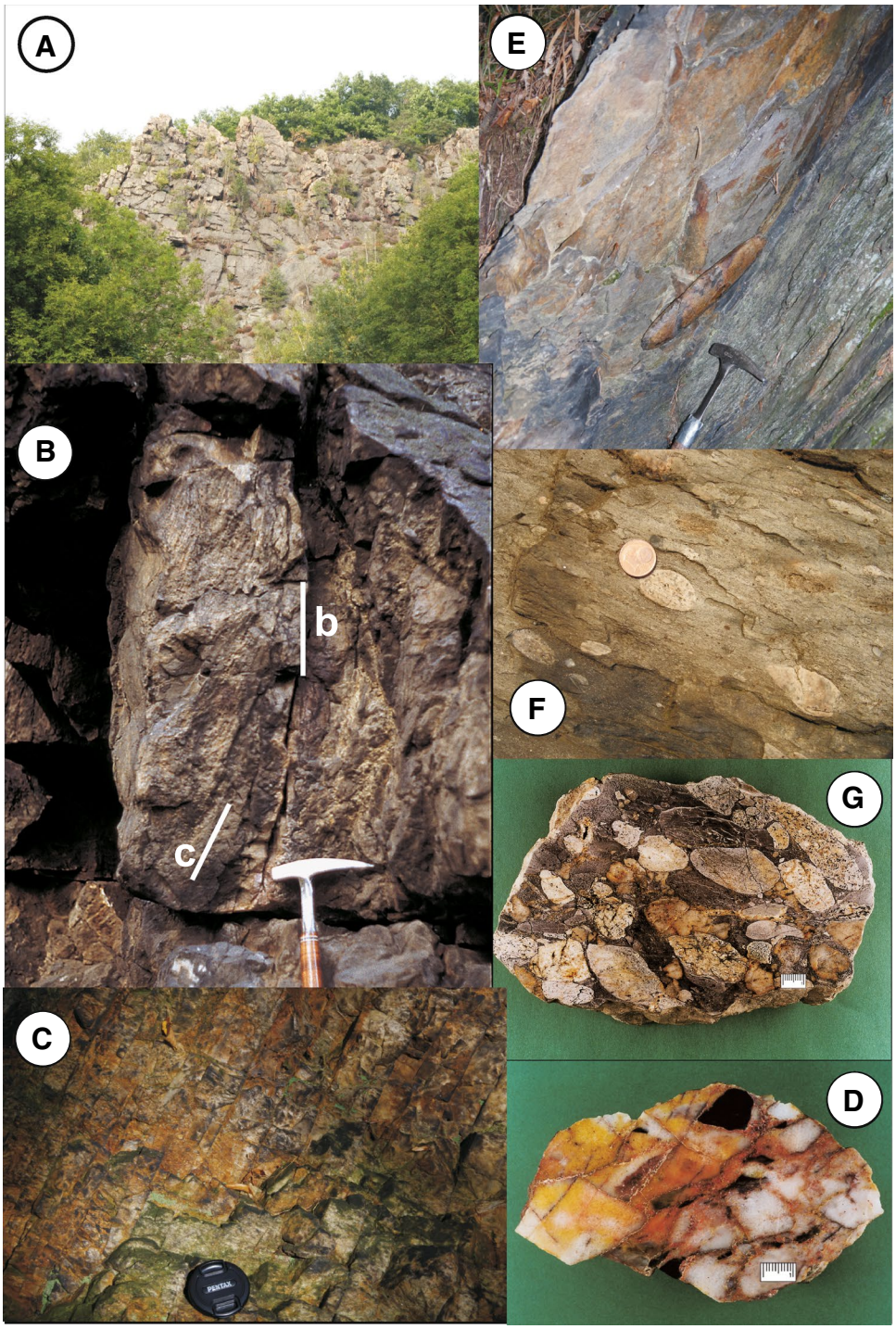


**Fig. 5** Outcrops and lithologies of the Weesenstein and Clanzschwitz groups. **a** Purpurberg quartzite member (Weesenstein group, Seidewitz formation) sub-vertically dipping and forming a ridge (cliffs of the Hallstein, Bahra valley, Elbtalschiefergebirge). **b** Purpurberg quartzite member, proximal thick-bedded facies, bedding is sub-vertical and shows ripple marks and cross bedding (Purpurberg near Friedrichswalde, Elbtalschiefergebirge, *c* cross bedding, *b* bedding plane), **c** Purpurberg quartzite member, distal thin-bedded facies, bedding is steeply dipping (outcrop in the "Röhrsdorfer Park" close to Röhrsdorf, Elbtalschiefergebirge). **d** Polished hand specimen of the conglomerate from the top-most part of the Purpurberg Quartzite member, white pebbles consist of quartzite, and black pebbles are composed of tourmaline hornfels (Purpurberg near Friedrichswalde, Elbtalschiefergebirge), **e** Isolated and tectonically stretched granitoid pebble in a matrix of greywacke and mudstone (Weesenstein group, Müglitz formation, "Weesenstein diamictite", klippen at the railway station Weesenstein, Müglitz valley, Elbtalschiefergebirge), **f** Isolated and tectonically stretched granitoid pebbles in a matrix of greywacke and mudstone (Weesenstein group, Müglitz formation, "Weesenstein diamictite", klippen at the footpath from Weesenstein to Köttewitz, Müglitz valley, Elbtalschiefergebirge), **g** Conglomerate of the Clanzschwitz group (member 3, North Saxon antiform)

studied elsewhere in the region (Talavera et al. 2015), the upper part could be earliest Cambrian in age.

A second deformation affected both the Lower and Upper Alcudian groups. The Upper Alcudian group may well represent a Cadomian remnant or successor basin deformed during the latest stage of the Cadomian orogeny. After final Cadomian deformation, a time of uplift, intense weathering, and erosion may represent the local response to the generalized rift event recorded everywhere in Iberia during the Cambrian–Lower Ordovician (Quesada 1991; Sánchez-García et al. 2003, 2008, 2010). Subsequent subsidence, interpreted in response to opening of the Rheic Ocean as a culmination of rifting, allowed the area to be transgressed in the Lower Ordovician establishing a new passive margin of Gondwana that survived until Variscan collision in the Devonian (Quesada 1991, 2006). The Lower

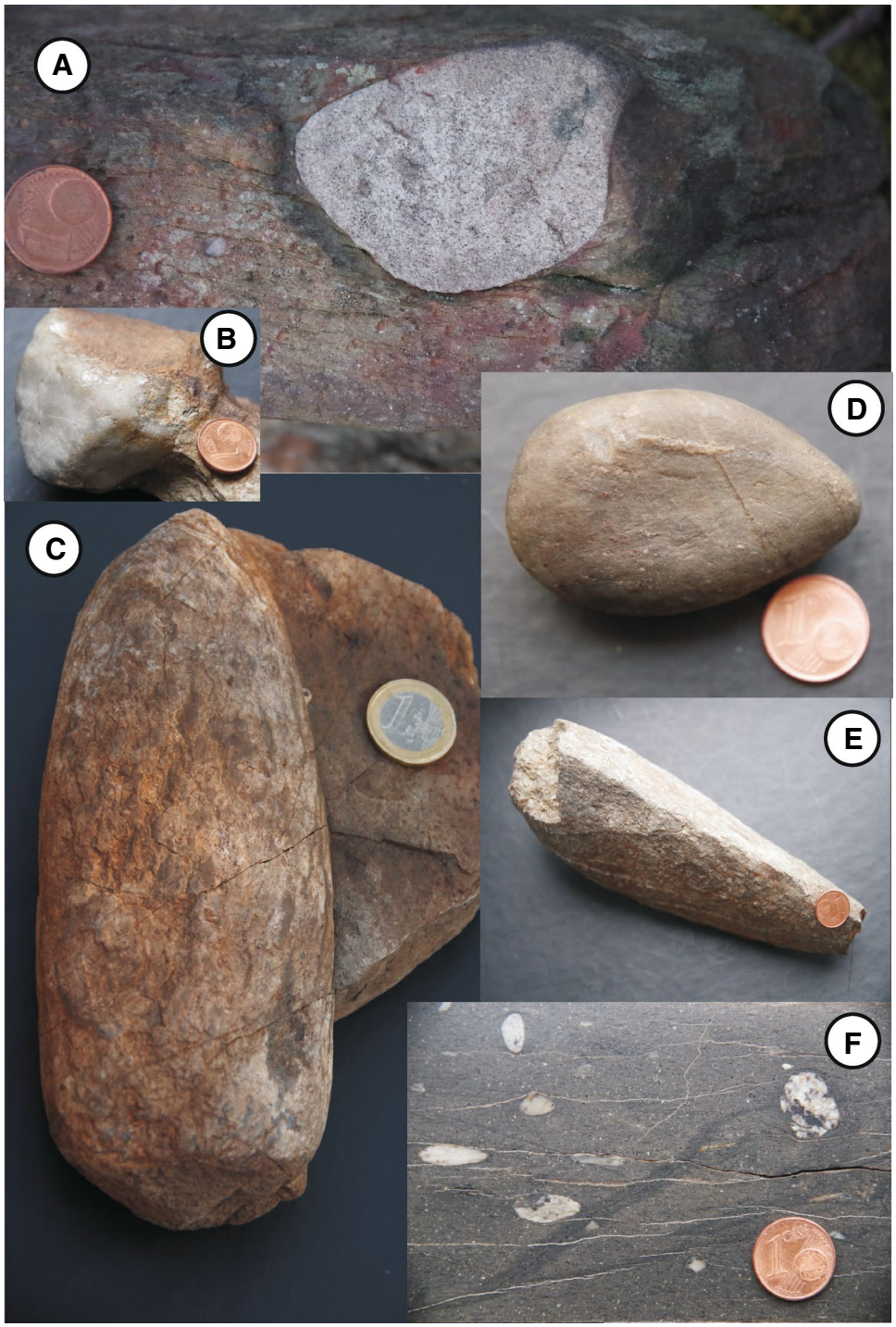


**Fig. 6** Images from the glaciomarine deposits of the Weesenstein group (Müglitz formation, klippen at the railway station Weesenstein, Müglitz valley, Elbtalschiefergebirge). **a** Granitoid dropstone in a rainout deposit, **b** dreikanter, **c** bullet shaped clast (flat iron-shaped pebble) in a rainout deposit (*upper part* sharp top formed by ice abrasion, *lower part* stump end in the pressure shadow during ice abrasion) ("*Bügeleisen-Geschiebe*"), **d** facetted and striated pebble (flat iron-shaped pebble = "*Bügeleisen-Geschiebe*"), **e** sharp facetted pebble from a rainout deposit, **f** rainout sediment showing isolated pebbles with different orientations "swimming" a fine-grained matrix

Ordovician-aged reddish sandstone and mudstone and the Armorican quartzite formation were the first to be deposited during this passive margin stage (Fig. 11; Pieren 2000).

Diamictites in the uppermost part the Lower Alcudian group (Figs. 11, 12) show distinct features indicative of a glaciomarine origin, including dropstones (Fig. 12b), rainout sediments (Fig. 12c), flat iron-shaped pebbles (*"Bügeleisen-Geschiebe"*) (Fig. 12d), and facetted pebbles (Fig. 12e). Pebble size varies between a few millimetres and 20 cm. Glaciomarine diamictite occur in c. 10–50 m-thick beds in the region of Orellana la Vieja, Orellana de la Sierra, and the Orellana reservoir (Embalse de Orellana; Pieren 2000).

## Samples for U–Pb dating and Hf isotope analyses

For our investigation to determine absolute age and provenance, we collected ten samples of clastic sedimentary rocks, six granodiorites, four granitoid pebbles, and one quartzite pebble. Pebbles were sourced from the glaciomarine diamictite layers in the Weesenstein and Clanzschwitz groups. One sample was taken from the Lower Alcudian group (Iberia) near Orellana. U–Pb LA–SF–ICP–MS* dating was carried out on zircons from all samples (*Laser ablation and inductively coupled plasma combined with a sector field mass spectrometer). Analysis of Hf isotopes by LA–MC–ICP–MS** was undertaken on zircon grains from Weesenstein and Clanzschwitz only (six sedimentary rock samples, three granitoid pebbles, one quartzite sample, and six granodiorite samples) (**Laser ablation and inductively coupled plasma combined with a multicollector mass spectrometer). The sample locations are marked in the columns and map of Figs. 4, 9 and 11. Exact location details are given in the headings of Table 1 (U–Pb ages) and Table 2 (Hf isotopes) (supplementary data).

The following sedimentary samples have been collected from the Müglitz formation of the Weesenstein group: WST1 (diamictite matrix, greywacke, Müglitz valley near Weesenstein, coordinates: N 50°56′09.77″; E 13°51′47.42″), GWQ1 (quartz wacke, Müglitz valley opposite to the castle in Weesenstein, coordinates: N 50°56′01.90″; E 13°51′34.80″), and W63d (conglomerate, Müglitz valley at the Fuchshübel, coordinates: N 50°56′23.21″; E 13°51′36.31″). From the Seidewitz formation (Purpurberg quartzite member) of the Weesenstein group, the quartzite sample P-Pur-1n-2-LA10 was collected (quartzite, top of the Purpurberg, coordinates: N 50°54′48.64″; E 13°54′23.03″). In addition, one quartzite pebble (WeG4) from the Müglitz formation was sampled (quartzite pebble, Müglitz valley at railway station Weesenstein, N 50°56′12.55″; E 13°51′49.67″). Furthermore, three granitoid pebbles from the diamictite in the Müglitz formation (Weesenstein group) were sampled: WeG2n, WeG3n, and WeG5 (granitoid pebbles, Müglitz valley at railway station Weesenstein, N 50°56′12.55″; E 13°51′49.67″). From the Dohna granodiorite, which is intrusive into the Weesenstein group, five samples were collected: Dohna1 (Müglitz valley, Köttewitzer Wehr, coordinates: N 50°56′29.12″; E 13°51′38.83″), Dohna2 (Müglitz valley, Köttewitzer Wehr, coordinates: N 50°56′29.28″; E 13°51′39.41″), Dohna 3 (Köttewitz, Müglitz valley on the foot path to Weesenstein, coordinates: N 50°56′33.25″; E 13°52′03.36″), Dohna 4 (roadcut near Dresden-Nickern and Goppeln, SE of the Gamighübel, temporary outcrop during road construction, coordinates: N 50°59′44.67″; E 13°46′28.07″), and DG1n (Bahra valley, coordinates: N 50°55′2.61″; E 13°54′41.60″.

From the Clanzschwitz group, two metasedimentary rock samples were sourced. The first sample (CL1) was taken from the matrix of the diamictite in member 3 (greywacke, Kleiner Steinberg near Clanzschwitz, coordinates: N 51°20′47.9″; E 13°09′41.5″. A second sample (CL2) came from the quartzite of member 2 (Großer Steinberg near Clanzschwitz, coordinates, N 51°21′1.17″; E 13°09′39.58″. A granitoid pebble (Cla 1n) from the diamictite (member 3) was sampled at the Schlangenberg near Wellerswalde (coordinates: N 51°20′44.01″; E 13°09′42.75″). From the Laas granodiorite that intruded the Clanzschwitz group, one sample was taken (Laas 1n, forest 1.5 km north of Clanzschwitz, N 51°21′34.34″; E 13°09′22.60″).

From the Lower Alcudian group, one sample of a diamictite matrix was taken from a road cut in the surroundings of Orellana (sample OR1, N 39°00′4.6″; W5°34′11.9″).

Hf isotope analysis by LA-MC- ICP-MS carried out on zircon grains from of five sedimentary rock samples (WST1, W63d, P-Pur-1b-2-LA10, CL1, and CL2), one quartzite pebble (WeG4), three granitoid pebbles (WeG2n, WeG5, Cla1n), and six granodiorite samples (Dohna 2, 3, 4, DG1n, Laas1).

## Methods

Zircon concentrates were separated from 2 to 4 kg samples at the Senckenberg Naturhistorische Sammlungen Dresden (Museum für Mineralogie und Geologie) by crushing (jaw crusher), sieving, heavy mineral separation by heavy liquid (LST), and by making use of a magnetic separator. Final selection of the zircon grains for U–Pb dating was achieved by hand-picking under a binocular microscope. Zircon grains of all grain sizes and morphological types were selected, mounted in resin blocks, and polished to half their thickness. Concerning stratigraphic ages, the stratigraphic time scale of Ogg et al. (2016) has been used.

### U–Th–Pb isotopes

Zircons ($n = 1124$) were analyzed for U, Th, and Pb isotopes by LA–SF ICP–MS techniques at the Museum für Mineralogie und Geologie (GeoPlasma Lab, Senckenberg Naturhistorische Sammlungen Dresden), using a Thermo-Scientific Element 2 XR sector field ICP-MS coupled to a New Wave UP-193 Excimer Laser System. A teardrop-shaped, low-volume laser cell was used to enable sequential sampling of heterogeneous grains (e.g., growth zones) during time resolved data acquisition. Each analysis consisted of approximately 15 s background acquisition followed by 30 s data acquisition, using a laser spot size of 25 and 35 µm, respectively. A common Pb correction based on the interference- and background-corrected $^{204}$Pb signal and a model Pb composition (Stacey and Kramers, 1975) was carried out if necessary. The necessity of the correction was

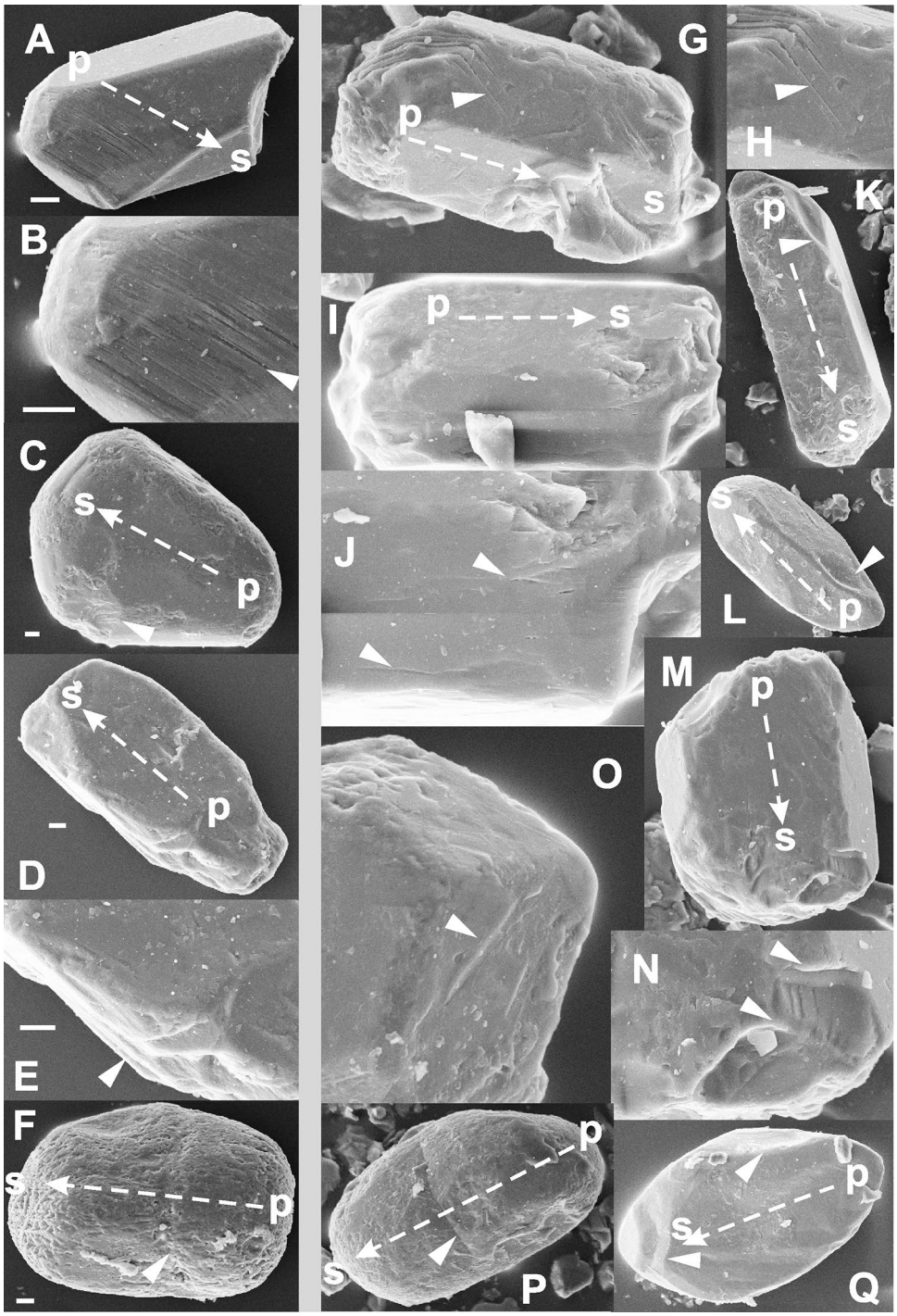


judged on whether the corrected $^{207}Pb/^{206}Pb$ lies outside of the internal error of the measured ratios. Discordant analyses were interpreted with care. Raw data were corrected for background signal, common Pb, laser induced elemental fractionation, instrumental mass discrimination, and time-dependant elemental fractionation of Pb/Th and Pb/U using an Excel® spreadsheet program developed by Axel Gerdes (Institute of Geosciences, Johann Wolfgang Goethe-University Frankfurt, Frankfurt am Main, Germany). Reported uncertainties were propagated by quadratic addition of the external reproducibility obtained from the standard zircon GJ-1 (~0.6 and 0.5–1% for the $^{207}Pb/^{206}Pb$ and $^{206}Pb/^{238}U$, respectively) during individual analytical sessions and the within-run precision of each analysis. According to the recommendation of Horstwood et al. (2016), a secondary zircon standard (Plesovice zircon) was analyzed. Sequences started with the analysis of five GJ1, one Plesovice, and ten unknowns followed by a repetition of a succession of three

◂**Fig. 7** SEM backscatter images of zircon grains affected by ice abrasion from a Quaternary glacial diamictite (**a**–**f** Germany, Isle of Rügen, coastline north of Saßnitz) and from a glaciomarine rainout deposit of the Weesenstein group (**g**–**q** sample WST 1, Müglitz formation). "p" indicates the assumed maximum pressure during ice abrasion and "s" the pressure shadow. *Arrows* show the resulting movement of the ice during abrasion processes. Images show examples of typical glacial features like high angularity, fresh faces, conchoidal breaks, and arc-step like fractures. **a** Scratches in a zircon grain. **b** Enlargement of **a**, **c** flat iron-shaped zircon grain. **d** zircon grain showing a more conic and a more stump end. **e** Scratches in the zircon grain shown in **d**. **f** Zircon grain illustrating shortening by compression, note the releasing band running perpendicular to the strain. **g** Zircon showing scratches (*left*) and rip-up structures (*right*), **h** enlargement of **g**. **i** Zircon showing rip-ups on the *right side*, which are sub-rounded by subsequent transport (see enlargement in **j**). **j** Enlargement of **i**, scratched zircon surface and sub-rounded edges of rip-ups, which rule out an origin during heavy mineral separation (e.g., by jaw crusher). **k** Zircon with relatively sharp top and stump end in the pressure shadow produced during ice abrasion., **l** zircon with rip-up showing sub-rounded edges. Similar to **k**, this grain hosts a sharp top and stump end in the pressure shadow produced during ice abrasion. **m** Zircon with rip-ups in the pressure shadow during ice abrasion. **n** Enlargement of M, zircon with rip-ups generated in the pressure shadow produced during ice abrasion; edges had been sub-rounded subsequently. **o** Zircon with scratches generated by ice abrasion. **p** Zircon grain showing shortening by compression, note the releasing band running perpendicular to the strain. **q** Flatiron-shaped zircon grain

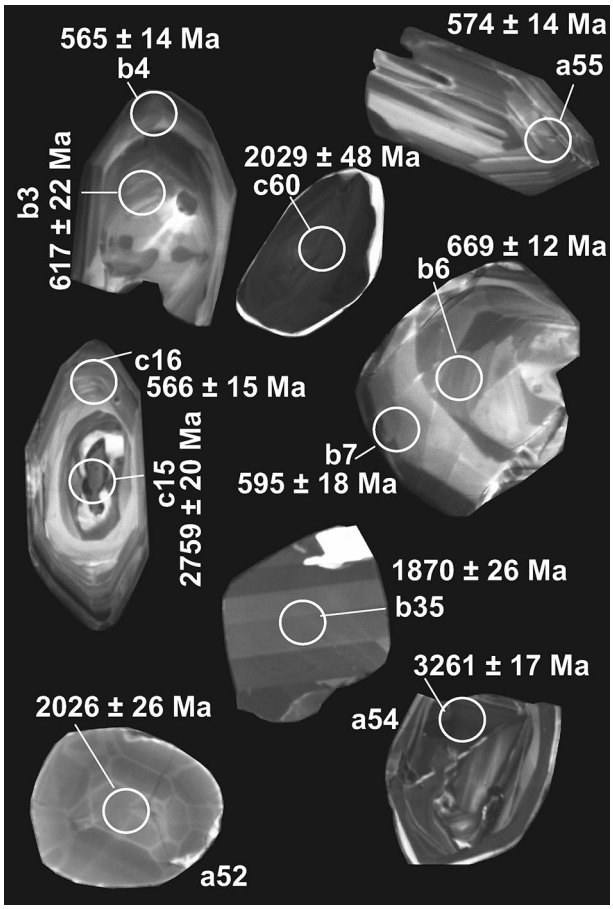


**Fig. 8** Cathodoluminescence (CL) images and U–Pb LA–ICP–MS ages of zircon grains from the Purpurberg Quartzite member (Seidewitz formation, Weesenstein group) (sample Pur 2). Complex zircon grains are very common (spots b3–b4; b6–b7; c15–c16). Zircon grains which were affected by high pressure metamorphism are frequent among the Eburnean-aged zircons (a52, c60). Very rare are zircon grains which originated in mafic melts (b35)

measurements of the GJ1 standard, one measurement of the Plesovice standard, and ten unknowns. U–Pb ages were in the recommended range of Sláma et al. (2008).

Concordia diagrams (2σ error ellipses) and Concordia ages (95% confidence level) were produced using Isoplot/Ex 2.49 (Ludwig 2001) and frequency and relative probability plots using AgeDisplay (Sircombe 2004). The $^{207}Pb/^{206}Pb$ age was taken for interpretation for all zircons >1.0 Ga, and the $^{206}Pb/^{238}U$ ages for younger grains. For further details on analytical protocol and data processing, see Gerdes and Zeh (2006). Th/U ratios are obtained from the LA–ICP–MS measurements of investigated zircon grains. U and Pb content and Th/U ratio were calculated relative to the GJ-1 zircon standard, and are accurate to approximately 10%. Analytical results of U–Th–Pb isotopes and calculated U–Pb ages are given in Table 1 (supplementary data).

### Lu–Hf isotopes

Hafnium isotope measurements on zircons ($n = 446$) were made using a Thermo-Finnigan Neptune multicollector ICP-MS at Goethe Universität Frankfurt (GUF, Institut für Geowissenschaften, Mineralogie) coupled to RESOlution M50 193 nm ArF Excimer laser system (Australian Scientific Instruments) following the method described in Gerdes and Zeh (2006, 2009). Spots of 40 µm in diameter were drilled with a repetition rate of 5.5 Hz and an energy density of 6 J/cm$^2$ during 50 s of data acquisition. The instrumental mass bias for Hf isotopes was corrected using an exponential law and a $^{179}Hf/^{177}Hf$ value of 0.7325. In case of Yb isotopes, the mass bias was corrected using the Hf mass bias of the individual integration step multiplied by a daily βHf/βYb offset factor (Gerdes and Zeh 2009). All data were adjusted relative to the JMC475 of $^{176}Hf/^{177}Hf$ ratio = 0.282160 and quoted uncertainties are quadratic additions of the within-run precision of each analysis and the reproducibility of the JMC475 (2SD = 0.0028%, $n = 8$). Accuracy and external reproducibility of the method were verified by repeated analyses of reference zircon GJ-1 and Plesovice. Results are in perfect agreement with previously published results (e.g., Gerdes and Zeh 2006; Sláma et al. 2008) and with the LA-MC-ICP MS long-term average of GJ-1 (0.282010 ± 0.000025; $n > 800$) and Plesovice (0.282483 ± 0.000025, $n > 300$) reference zircon at GUF.

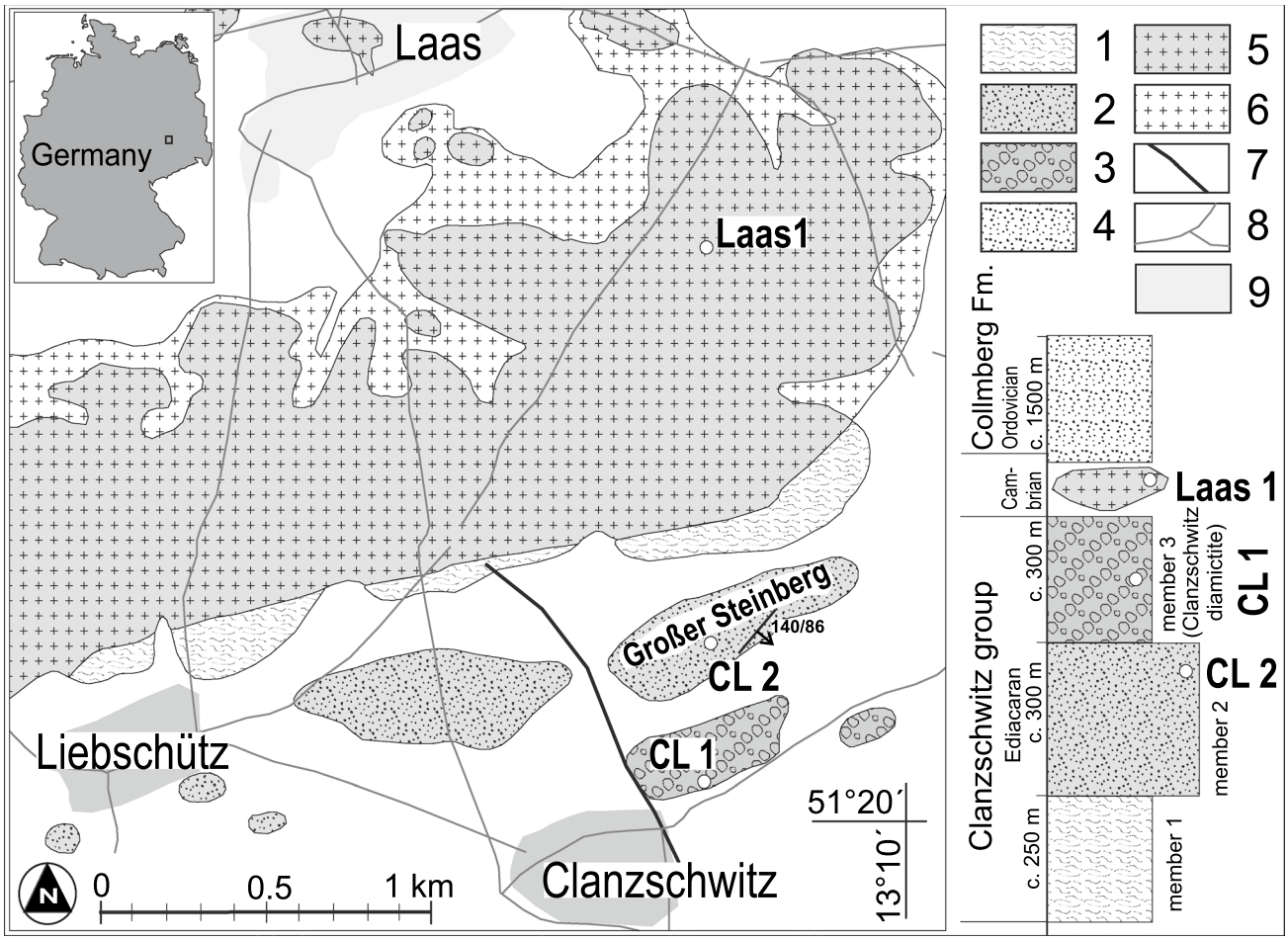


**Fig. 9** Geological map with sample locations and a lithostratigraphic column of the Clanzschwitz group (North Saxon antiform). *1* Mudstones and quartz schists affected by contact metamorphism of the Laas granodiorite with large andalusite crystals (up to 1 cm) (member 1 of the Clanzschwitz group), *2* quartzite and quartz schist (member 2), *3* diamictite (glaciomarine diamictite, "Clanzschwitz tillite") (member 3), *4* quartzite and quartz schist (Ordovician, Collmberg formation), *5* Laas granodiotite, *6* Laas granodiorite with a gneissic texture, *7* fault, *8* roads, and *9* villages

The initial $^{176}Hf/^{177}Hf$ values are expressed as εHf(t), which is calculated using a decay constant value of $1.867 \times 10^{-11}$ year$^{-1}$, CHUR after Bouvier et al. (2008, $^{176}Hf/^{177}Hf_{CHUR,today} = 0.282785$ and $^{176}Lu/^{177}Hf_{CHUR,today} = 0.0336$) and U–Pb and Pb–Pb ages obtained for the respective domains (Table 2, supplementary data). For the calculation of Hf two stage model ages ($T_{DM}$) in billion years, the measured $^{176}Lu/^{177}Lu$ of each spot (first stage = age of zircon), a value of 0.0113 for the average continental crust, and a juvenile crust $^{176}Lu/^{177}Lu_{NC} = 0.0384$ and $^{176}Hf/^{177}Hf_{NC} = 0.283165$ (average MORB; Chauvel et al. 2008) were used.

Cathodoluminescence (CL, supplementary data) and backscatter images were made using an EVO 50 scanning electron microscope (Zeiss) at Senckenberg Naturhistorische Sammlungen Dresden.

## Results and discussion

### Age constraints for glaciomarine sedimentation

U–Pb ages of detrital zircons are represented in Figs. 13 and 14. Because ash beds and fossils have not been found in the investigated sections, the maximum depositional age (MDA) had to be used for the stratigraphic age determination (Condon and Bowring 2011).

The maximum depositional age for each sample was calculated from the youngest zircon population for each sandstone sample (Figs. 13, 14). For the Weesenstein diamictite (WST1, Müglitz formation, Weesenstein group), a maximum depositional age of 562 ± 5 Ma was obtained (Fig. 13). Underlying strata show similar maximum depositional ages of 562 ± 5 Ma for the Purpurberg quartzite

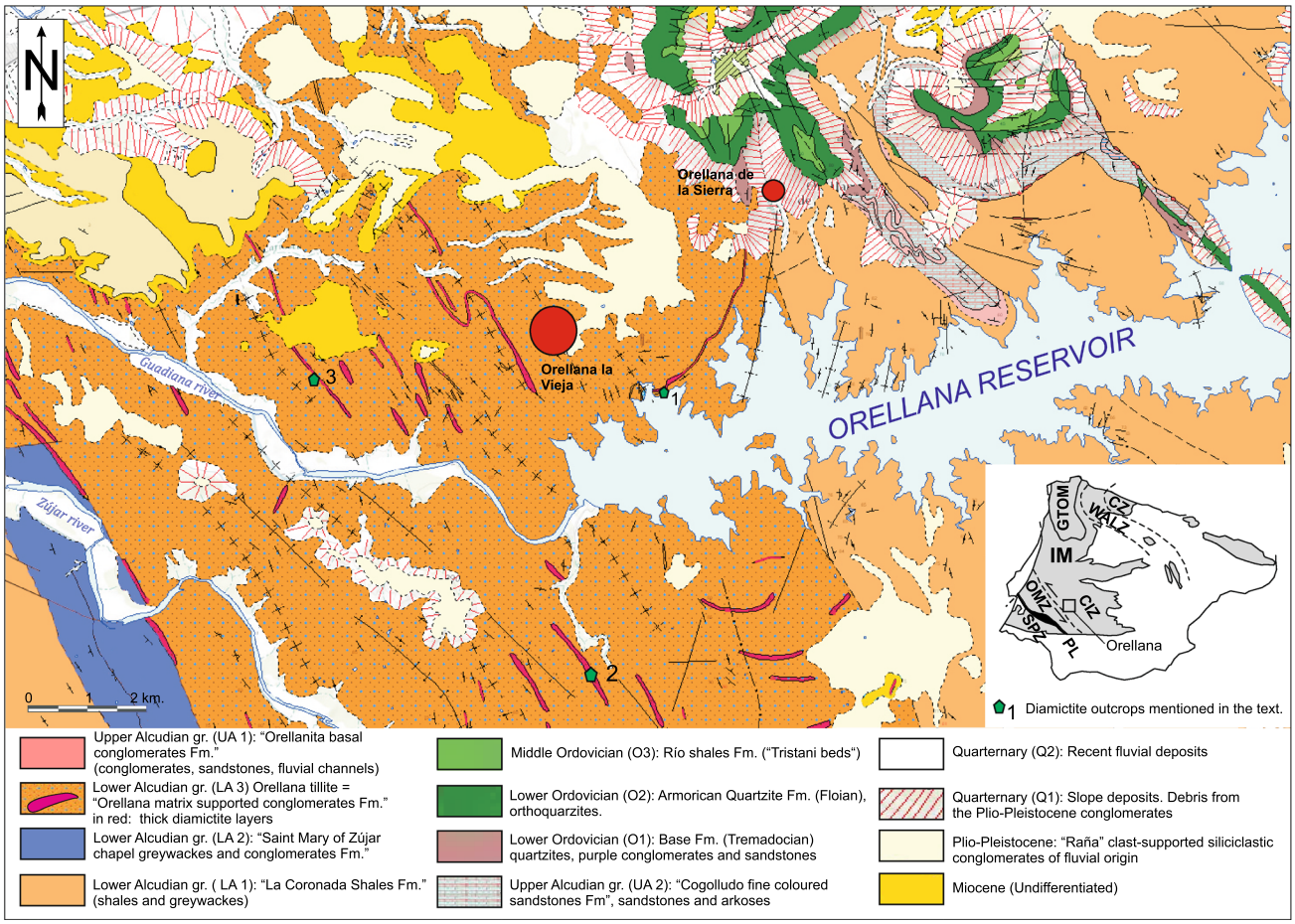


**Fig. 10** Geological map of a part of the Alcudia antiform at the Orellana reservoir (Orellana region, Central Iberian zone, Iberia) (from García-Hidalgo et al. 1993; Pieren 2000; Clariana García et al. 2017). Locality 1: waterline of the sweetwater reservoir (images see Fig. 12), N 39°00′8.4″; W5°31′18.9″. Locality 2: roadcut near Orellana (images see Fig. 12), N 38°52′52.8″; W5°29′5.6″. Locality 3: roadcut near Orellana, sample location of OR-1 (images see Fig. 12), N 39°00′4.6″; W5°34′11.9″. *Red dots* are towns. *Inset map CIZ* Central Iberian zone, *CZ* Cantabrian zone, *GTOM* Galicia-Tras os Montes zone, *MZ* Moldanubian zone, *OMZ* Ossa-Morena zone, *PL* Pulo do Lobo zone, *SPZ* South Portuguese zone

member and 564 ± 5 Ma for quartz wacke sample GWQ1. Three granitoid pebbles from the diamictite horizons in the Müglitz formation exhibit ages of 576 ± 7, 572 ± 2, and 566 ± 4 Ma (Fig. 15), and support the maximum depositional age obtained from detrital zircon. The upper limit (minimum age) for the deposition of the Weesenstein diamictite is estimated based on the age of intrusion of the Dohna granodiorite (538 ± 2 Ma, Fig. 16).

The Clanzschwitz diamictite (CL1, member 3, Clanzschwitz group) exhibits a maximum depositional age of 570 ± 8 Ma supported by another age determination based on a zircon from the underlying member 2 (CL2), which is 565 ± 5 Ma (Fig. 14). The age of a zircon in the granitoid pebble taken from the diamictite (member 3, Cla1n) is 574 ± 5 Ma (Table 1, supplementary data). The intrusion age of the Laas granodiorite (537 ± 5, Fig. 16) offers the minimum age for the deposition of the Clanzschwitz diamictite.

The zircons from the Orellana diamictite (OR1) in the Lower Alcudian group of the Central Iberian zone yielded a maximum depositional age of 565 ± 4 Ma (Fig. 14).

In all three cases (Weesenstein, Clanzschwitz, and Orellana), the maximum depositional age for the diamictites is significantly younger than that for the Gaskiers glaciation in Newfoundland and in SE New England (Squantum). Thus, the three diamictites should represent a post-Gaskiers glacial event during Ediacaran time. Alternatively, a shifting of the icecenter from Avalonia (Gaskiers glaciation, c. 579–581 Ma) to West African peri-Gondwana (Weesenstein-Orellana glaciation, c. 565 Ma) over time

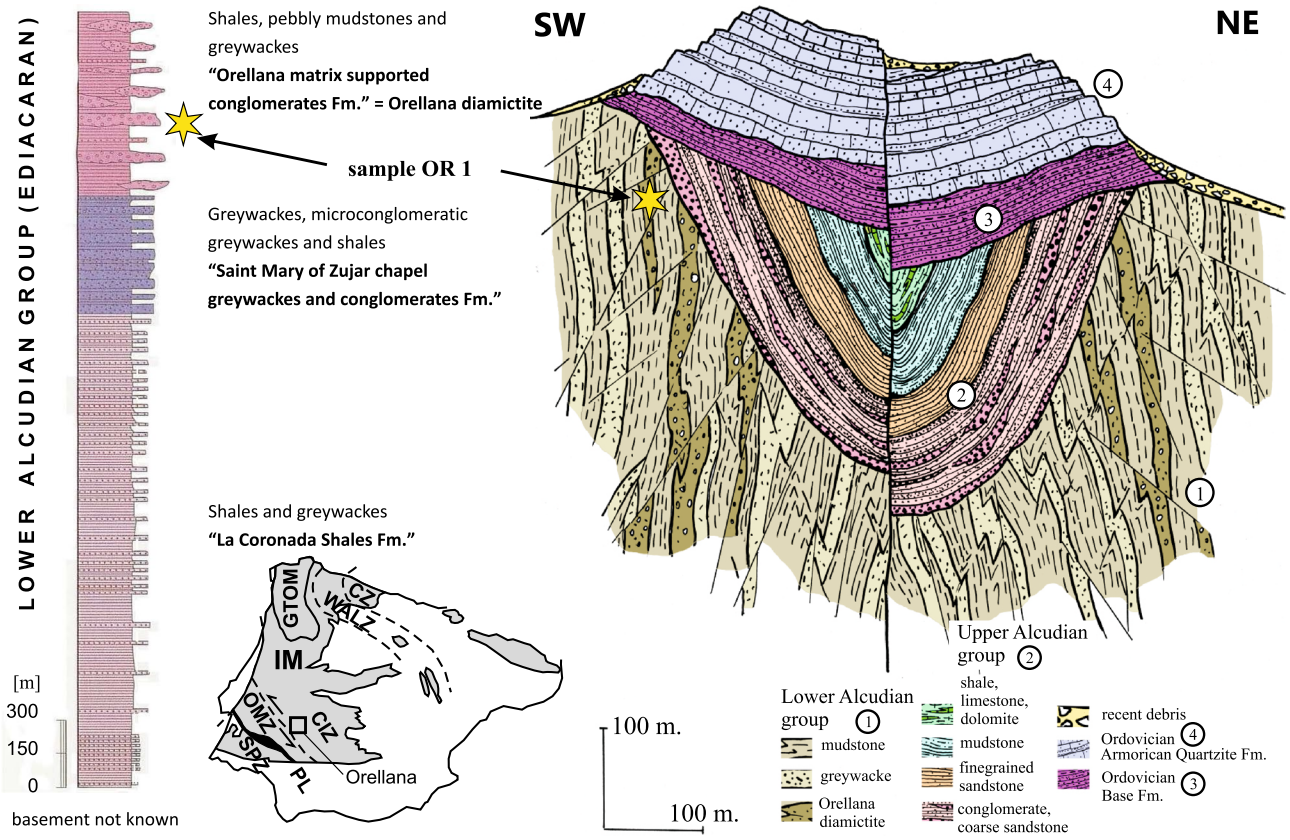


**Fig. 11** Idealized section of the Lower and Upper Alcudian groups (Alcudian supergroup) and overlying Ordovician strata from the Alcudia antiform near Orellana (Central Iberian zone, Spain). *Left* stratigraphic log of the Lower Alcudian group) (from García-Hidalgo et al. 1993; Pieren 2000). For abbreviations of inset, see Fig. 10

would be possible. However, this solution seems to be more unlikely because of the existence of contemporaneous occurence of c. 565 Ma glacial deposits in Virginia (Hebert et al. 2010).

## Provenance and crustal growth of the hinterland

U–Pb ages and Hf isotopes are classical tools for provenance studies and analysis of tectonomagmatic events, important for our understanding of patterns of crustal growth in the hinterland. Information of the pre-glacial hinterland can be obtained from the detrital zircon of quartzite pebble WeG4 taken from the Weesenstein diamictite, with a maximum age of deposition being 612 ± 7 Ma (Fig. 14). Because younger zircons aged at c. 565–600 Ma are lacking, it could not have been derived from the Purpurberg quartzite member, which underlies the diamictites of the Müglitz formation. Instead, the pebble must be derived from much older strata and, therefore, representative of the sedimentary cover of the paleolandscape in the hinterland at c. 600–610 Ma. The detrital zircon populations derived from the pebble exhibit a dominant peak at 630 Ma and a number of secondary peaks of Neoproterozoic age at c. 710 and 790 Ma. No Tonian and Mesoproterozoic zircons were found. Palaeoproterozoic zircon dates range between c. 1769 ± 66 and 2471 ± 13 Ma, while the Archaean zircon population occupies the range of 2525 ± 59 to 3163 ± 26 Ma (Fig. 14). Such a pattern of the zircon population is typical for peri-Gondwanan deposits originating in the periphery of the West African craton (Linnemann et al. 2014). A pronounced peak ranging from 1942 ± 18 to 2168 ± Ma is coeval with the so-called Eburnean orogeny. Neoproterozoic zircons came from one of the Pan-African orogens. The latter ones formed during continent–continent collision of the amalgamation of the Gondwana supercontinent at c. 610–630 Ma (Black et al. 1994). All in all, the zircon population found in the quartzite pebble from the Weesenstein tillite (Müglitz formation) represents the composition of rocks in a pre-glacial hinterland,

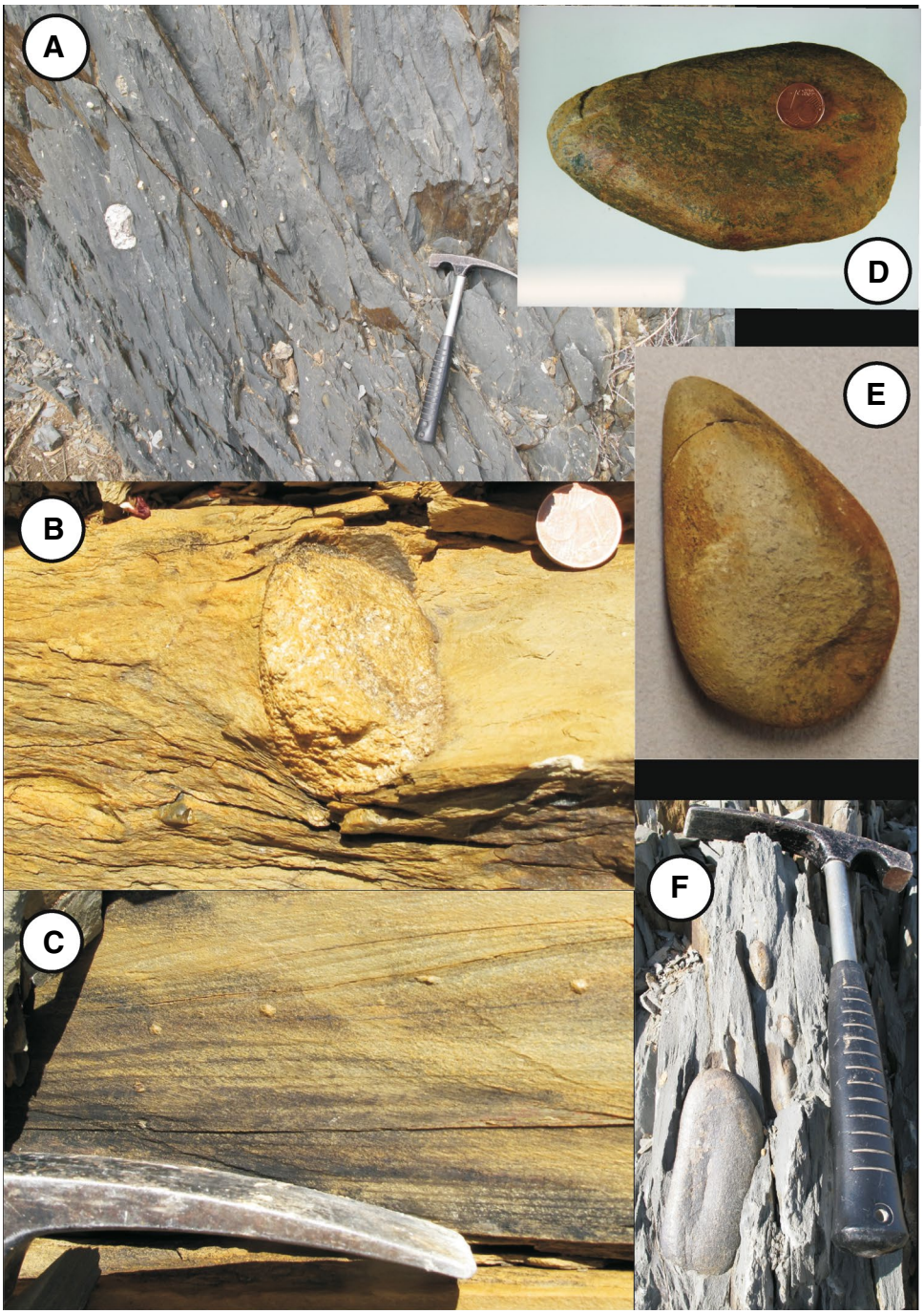


**Fig. 12** Images from the glaciomarine deposits of the Lower Alcudian group ("Orellana diamictite", Alcudia antiform, Central Iberian zone, Spain). **a** Diamictite containing pebbles of sedimentary rocks (quartzite, greywacke) (Locality 2, Fig. 10), **b** dropstone in a rainout deposit, **c** rainout deposit with millimetre-sized rock fragments, **d** faceted and flat iron-shaped pebble in a rainout deposit (flat faceted top and sharp left end formed by ice abrasion; stump right end formed in the pressure shadow during ice abrasion ("*Bügeleisen-Geschiebe*") (Locality 3, Fig. 10), **e** Facetted pebble from a rainout deposit (flat iron-shaped pebble = "*Bügeleisen-Geschiebe*") (Locality 3, Fig. 10), and **f** large flat iron-shaped pebble (="*Bügeleisen-Geschiebe*"), a fine-grained diamictite matrix. (**b**, **c**, **f** images photographed in a roadcut at Casa el Canchal, N 38°52′52.8″; W5°29′5.6″)

which consisted of eroded parts of the Pan-African orogen and the West African craton. In this region, no Mesoproterozoic zircon grains were found.

All samples of clastic sediments from the Weesenstein, Clanzschwitz, and Orellana areas show a very similar pattern of zircon populations (Figs. 13, 14) typical for Cadomia and its West African hinterland (Linnemann et al. 2014). The U–Pb ages of the detrital zircons from this study can be grouped in three major groups: (1) the Neoproterozoic zircons (c. 565–950 Ma), the Palaeoproterozoic zircons (c. 1800–2200 Ma), and the Archaean zircons (c. 2500–3600 Ma). In addition, some samples of siliciclastic sedimentary rocks yielded a few Mesoproterozoic zircon grains (c. 1000–1200 and c. 1550 Ma). The Palaeoproterozoic and Archaean pattern is typical of a West African Craton provenance (e.g., Linnemann et al. 2000, 2014; Abati et al. 2010, 2012). Neoproterozoic zircon populations are diagnostic of provenance from the Cadomian orogen and

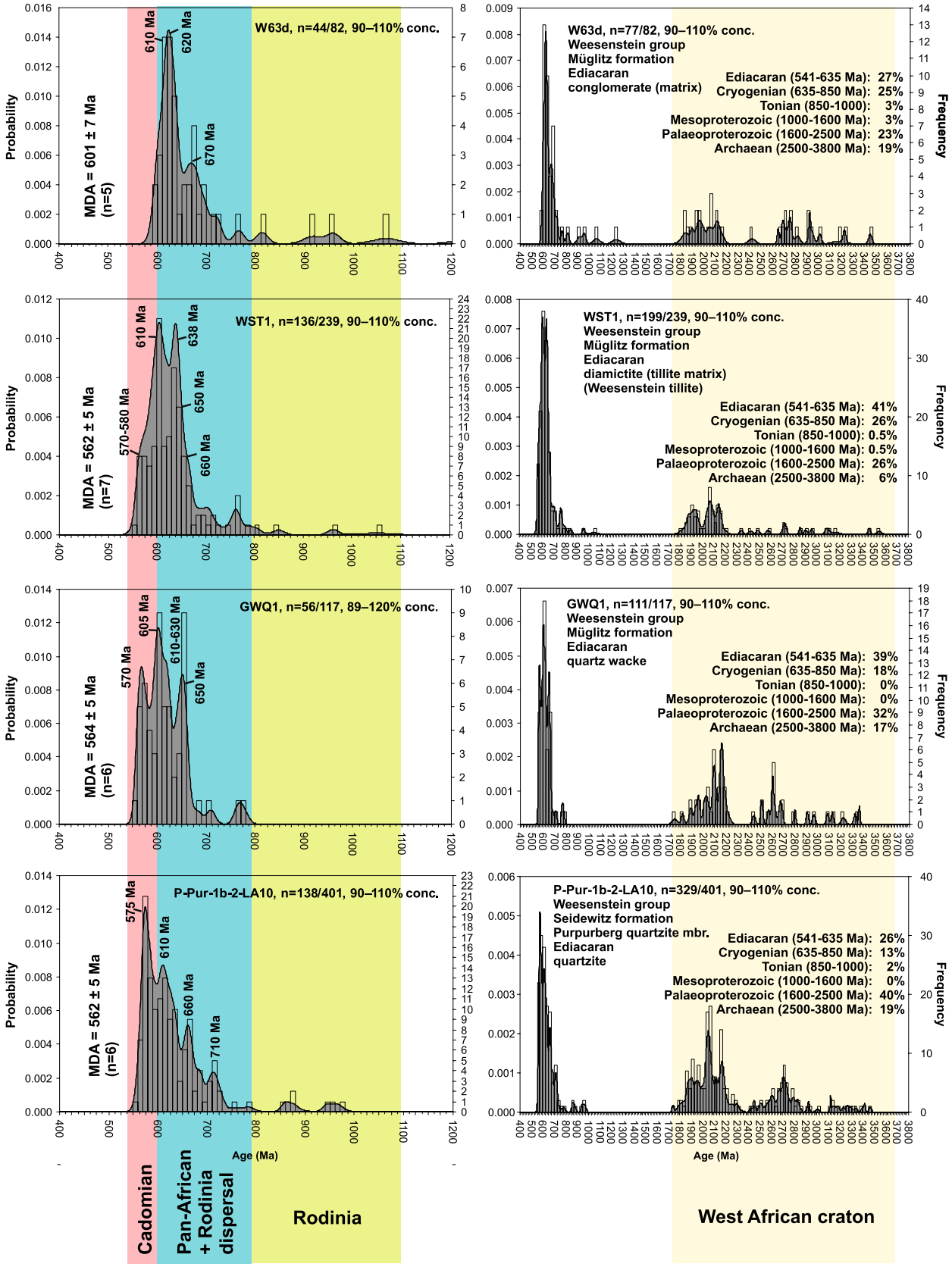
W63d, n=44/82, 90–110% conc.
MDA = 601 ± 7 Ma (n=5)
610 Ma
620 Ma
670 Ma
W63d, n=77/82, 90–110% conc.
Weesenstein group
Müglitz formation
Ediacaran
conglomerate (matrix)
Ediacaran (541-635 Ma): 27%
Cryogenian (635-850 Ma): 25%
Tonian (850-1000): 3%
Mesoproterozoic (1000-1600 Ma): 3%
Palaeoproterozoic (1600-2500 Ma): 23%
Archaean (2500-3800 Ma): 19%
WST1, n=136/239, 90–110% conc.
MDA = 562 ± 5 Ma (n=7)
570-580 Ma
610 Ma
638 Ma
650 Ma
660 Ma
WST1, n=199/239, 90–110% conc.
Weesenstein group
Müglitz formation
Ediacaran
diamictite (tillite matrix)
(Weesenstein tillite)
Ediacaran (541-635 Ma): 41%
Cryogenian (635-850 Ma): 26%
Tonian (850-1000): 0.5%
Mesoproterozoic (1000-1600 Ma): 0.5%
Palaeoproterozoic (1600-2500 Ma): 26%
Archaean (2500-3800 Ma): 6%
GWQ1, n=56/117, 89–120% conc.
MDA = 564 ± 5 Ma (n=6)
570 Ma
605 Ma
610-630 Ma
650 Ma
GWQ1, n=111/117, 90–110% conc.
Weesenstein group
Müglitz formation
Ediacaran
quartz wacke
Ediacaran (541-635 Ma): 39%
Cryogenian (635-850 Ma): 18%
Tonian (850-1000): 0%
Mesoproterozoic (1000-1600 Ma): 0%
Palaeoproterozoic (1600-2500 Ma): 32%
Archaean (2500-3800 Ma): 17%
P-Pur-1b-2-LA10, n=138/401, 90–110% conc.
MDA = 562 ± 5 Ma (n=6)
575 Ma
610 Ma
660 Ma
710 Ma
P-Pur-1b-2-LA10, n=329/401, 90–110% conc.
Weesenstein group
Seidewitz formation
Purpurberg quartzite mbr.
Ediacaran
quartzite
Ediacaran (541-635 Ma): 26%
Cryogenian (635-850 Ma): 13%
Tonian (850-1000): 2%
Mesoproterozoic (1000-1600 Ma): 0%
Palaeoproterozoic (1600-2500 Ma): 40%
Archaean (2500-3800 Ma): 19%
Probability
Frequency
Age (Ma)
Cadomian
Pan-African + Rodinia dispersal
Rodinia
West African craton

◂**Fig. 13** Combined binned frequency and probability density distribution plots of U–Pb LA–ICP–MS ages of detrital zircon grains from the Weesenstein group (Ediacaran of the Elbe zone) in the ranges of 400–1200 Ma (*left*) and 400 to 3800 Ma (*right*): W63d (conglomerate, Müglitz formation), WST1 (diamictite matrix, greywacke, Müglitz formation), GWQ1 (quartz wacke, Müglitz formation), and P-Pur1b-2-LA10 (quartzite, Purpurberg quartzite member, Seidewitz formation); *MDA* maximum depositional age

from the Pan-African basement of the Trans-Saharan Belt or a related area (Linnemann 2007, Linnemann et al. 2011; Drost et al. 2011). The scarce Mesoproterozoic zircons might well have been derived from the cratonic neighbours of the West African Craton, which were at c. 570 Ma the Amazonian or Sub-Saharan cratons (e.g., Gärtner et al. 2013).

The pre-glacial deposits of the Purpurberg quartzite member (Seidewitz formation, Weesenstein group) and of member 2 of the Clanzschwitz group show a much stronger sedimentary input from the cratonic hinterland indicated by the strong Palaeoproterozoic and Archaean zircon populations (Figs. 13, 14).

Detrital zircon populations in the range of c. 565–580 Ma in our samples of sedimentary rocks and granitoid pebbles aged at c. 566–576 Ma indicate that the main peak of the Cadomian orogeny was over and the Cadomian orogen was exposed during the time of glacial processes.

Similarities of the zircon populations of glacigenic and related sedimentary rocks from Bohemia and Iberia document no differences in the composition of the West African hinterland and a coeval plate tectonics evolution. The relative large distance of about 1800 km between the glacial diamictites in Bohemia and Iberia constrains a relative wide distribution of the glaciated area within the Cadomian orogen.

Neoproterozoic zircons of glacial deposits and related rocks from the Saxo-Thuringian zone show a wide variability of the epsilon Hf ($\varepsilon$Hf) values, in the range of 13 and −41 (Fig. 17). About 15% have positive ($\varepsilon$Hf). Such an initial epsilon Hf notation indicates that these zircons crystallized either from magmas directly derived from a depleted mantle source (=juvenile magmas) contaminated with different amounts of older crust or by partial melting of a relatively juvenile crust of a Cadomian or Pan-African magmatic arc affinity, respectively (Fig. 17). Zircons close to the depleted mantle array are very scarce and about 660–690 Ma old (Fig. 17), which is in line with the early magmatic arc setting in the Pan-African orogens. Most zircon with ages of c. 540–700 Ma has lower $\varepsilon$Hf (up to −41), suggesting that juvenile magmas were contaminated by older crust or recycling of the juvenile island arcs together with some older crust (Fig. 17). About 85% of Neoproterozoic zircon show negative $\varepsilon$Hf. Zircons aged between ca. 540 and 700 Ma with negative $\varepsilon$Hf, in the range of −7 to −21, and model ages between c. 1.7 and 2.2 Ga can be explained by almost pure reworking of older Eburnean crust (Fig. 17). Surprisingly, eleven Neoproterozoic zircon grains show more negative $\varepsilon$Hf between −20 and −41. Such zircons lie on a linear array with most Eburnean and Archaean zircons, and may have been formed by recycling of c. 2500–3800 Ma old Archaean crust (Fig. 17). The relatively abundant group with negative and moderate positive $\varepsilon$Hf (+8 to −8) is only compatible with mixing of the newly formed Cadomian crust at c. 540–700 Ma and of Eburnean and Archaean crust (see mixing field in Fig. 17). Zircons within the c. 537–540 Ma age group of old granodiorites of Laas and Dohna show a spread of the $\varepsilon Hf_i$ in the range of +2 to −17 and fall in the same mixing field. Thus, Cadomian granitoid magmatism seems to be derived from an evolved Cadomian crust (Fig. 17).

From Mesoproterozoic zircon grains, only four analyses could be performed. Three of them point to the recycling of a Palaeoproterozoic crust, and one could be derived from the recycling of a true Mesoproterozoic crust (Fig. 17). Palaeoproterozoic zircons (c. 1.7–2.4 Ga), in most cases, exhibit $\varepsilon$Hf of +8 to −10 and model ages of about 2.0 and 2.7 Ga (Fig. 17). Such grains document a recycling of Palaeoproterozoic and Neoarchean crust. A number of zircon grains have positive $\varepsilon$Hf notations. Some of them fall on the depleted mantle curve. These zircons show a strong affinity to a juvenile Eburnean crust. Other Palaeoproterozoic zircon grains are characterized by $\varepsilon$Hf of −10 to −26 (Fig. 17). These zircons demonstrate a recycling of a ca. 3.0–3.8 Ga old Archean crust. Two Palaeoproterozoic zircons from the Purpurberg quartzite member are exceptional. These two zircons are 2056 ± 34 and 2103 ± 40 Ma old, and show a strongly negative $\varepsilon$Hf of −34 and −32 (Fig. 17). Calculated $T_{DM}$ model ages are 4.27 and 4.21 Ga, respectively. Both grains lie on a linear array parallel to the $^{176}Lu/^{177}Hf$ evolution of a continental crust extracted from the depleted mantle during the Hadean that mirrors a Jack Hills Trend (Fig. 17), named after the location of the oldest zircon on Earth (Wilde et al. 2001). U–Pb ages combined with Hf isotope data demonstrate that a c. 4.2–4.3 Ga old crust must have survived in the framework of the West African Craton at least until c. 2.05–2.1 Ga ago.

Most Neo- to Palaeoarchaean zircon grains dated at 2.5 to 3.5 Ga exhibit $\varepsilon$Hf values between +4 and −18 with expecting model ages of 2.7–3.7 Ga (Fig. 17). Neo- to Palaeoarchaean crustal evolution points to the recycling of late Neo- to Eoarchean crust of the West African Craton. $T_{DM}$ model ages indicate three different Archean crustal domains, which would have been recycled. These

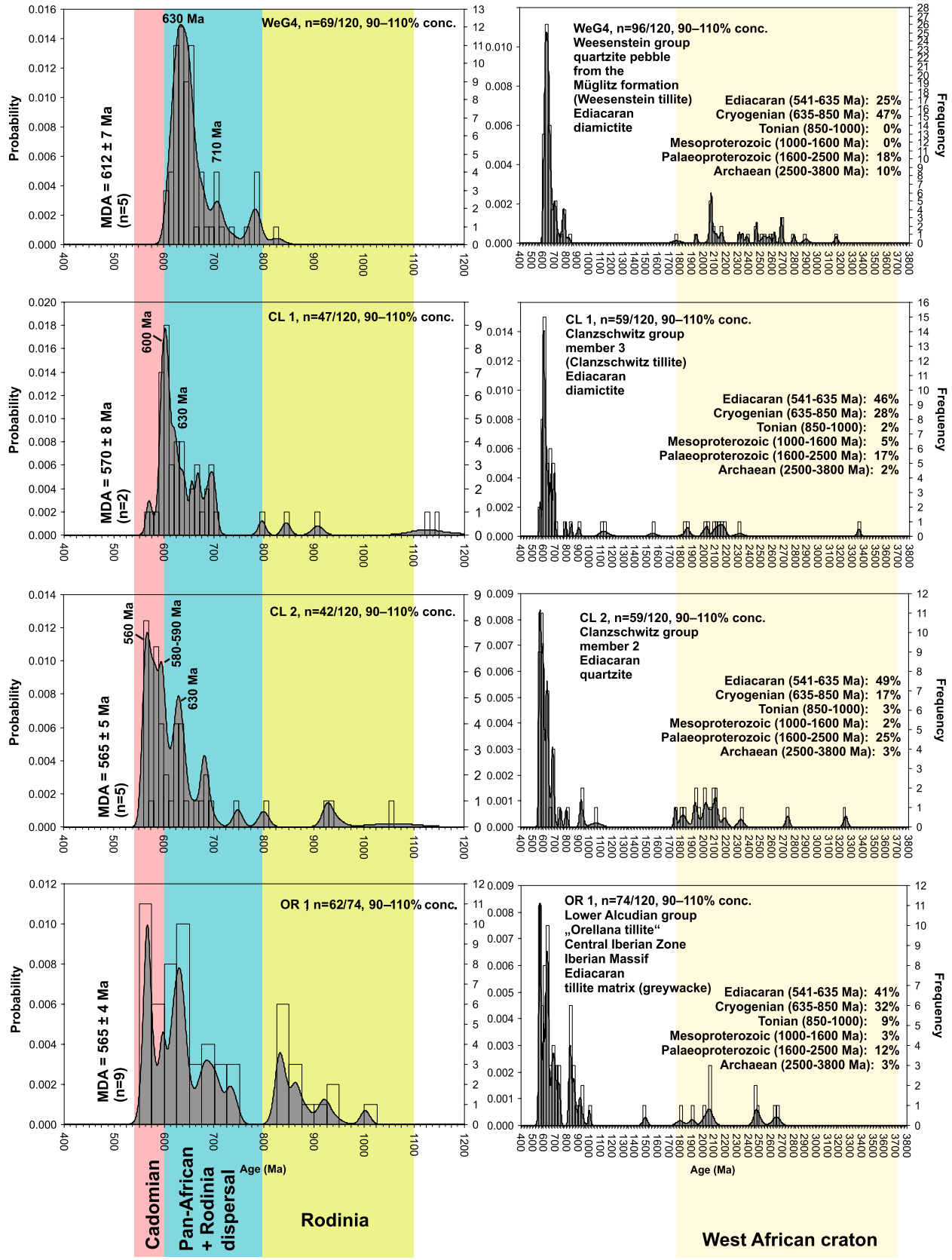
WeG4, n=69/120, 90–110% conc.
630 Ma
710 Ma
MDA = 612 ± 7 Ma (n=5)
WeG4, n=96/120, 90–110% conc.
Weesenstein group quartzite pebble from the Müglitz formation (Weesenstein tillite) Ediacaran diamictite
Ediacaran (541-635 Ma): 25%
Cryogenian (635-850 Ma): 47%
Tonian (850-1000): 0%
Mesoproterozoic (1000-1600 Ma): 0%
Palaeoproterozoic (1600-2500 Ma): 18%
Archaean (2500-3800 Ma): 10%
CL 1, n=47/120, 90–110% conc.
600 Ma
630 Ma
MDA = 570 ± 8 Ma (n=2)
CL 1, n=59/120, 90–110% conc.
Clanzschwitz group member 3 (Clanzschwitz tillite) Ediacaran diamictite
Ediacaran (541-635 Ma): 46%
Cryogenian (635-850 Ma): 28%
Tonian (850-1000): 2%
Mesoproterozoic (1000-1600 Ma): 5%
Palaeoproterozoic (1600-2500 Ma): 17%
Archaean (2500-3800 Ma): 2%
CL 2, n=42/120, 90–110% conc.
560 Ma
580-590 Ma
630 Ma
MDA = 565 ± 5 Ma (n=5)
CL 2, n=59/120, 90–110% conc.
Clanzschwitz group member 2 Ediacaran quartzite
Ediacaran (541-635 Ma): 49%
Cryogenian (635-850 Ma): 17%
Tonian (850-1000): 3%
Mesoproterozoic (1000-1600 Ma): 2%
Palaeoproterozoic (1600-2500 Ma): 25%
Archaean (2500-3800 Ma): 3%
OR 1 n=62/74, 90–110% conc.
MDA = 565 ± 4 Ma (n=9)
OR 1, n=74/120, 90–110% conc.
Lower Alcudian group „Orellana tillite“ Central Iberian Zone Iberian Massif Ediacaran tillite matrix (greywacke)
Ediacaran (541-635 Ma): 41%
Cryogenian (635-850 Ma): 32%
Tonian (850-1000): 9%
Mesoproterozoic (1000-1600 Ma): 3%
Palaeoproterozoic (1600-2500 Ma): 12%
Archaean (2500-3800 Ma): 3%
Probability
Frequency
Age (Ma)
Cadomian
Pan-African + Rodinia dispersal
Rodinia
West African craton

◂**Fig. 14** Combined binned frequency and probability density distribution plots of U–Pb LA–ICP–MS ages of detrital zircon grains from the Weesenstein, Clanzschwitz, and Lower Alcudian groups (Ediacaran) in the ranges of 400–1200 Ma (*left*) and 400–3800 Ma (*right*): WeG4 (quartzite pebble from the Weesenstein diamictite, Ediacaran, Müglitz formation, Weesenstein group, Elbe zone), CL1 (diamictite matrix, Ediacaran, Clanzschwitz group, member 3, North Saxon antiform), CL2 (quartzite, Ediacaran, Clanzschwitz group, member 2, North Saxon antiform), and OR1 (greywacke, diamictite matrix, Ediacaran, Orellana diamictite, Lower Alcudian group, Central Iberian zone, Spain)

units are characterized by model ages of c. 3.0, 3.2–3.3, and 3.5–3.7 Ga, respectively. Most known West African Archean ages of granitoid magmatism fall between c. 2.7 and 3.0 Ga (e.g. Rocci et al. 1991). Scarce occurrence of 3.42–3.52 Ga old felsic rocks in the Amsaga area (Mauritania) has been reported by Potrel et al. (1996, 1998). It is very obvious, that both, Liberian (c.3.0 Ga) and Leonian (c. 3.4 Ga) crust, were recycled during Archaean time.

## Conclusions

Sedimentary features, aspects of basin development, plate tectonics framework, U–Pb ages, and Hf isotope data together allow reconstruction of Ediacaran glacial processes, palaeogeography, timing of orogenic processes, and crustal growth of the piece of the Cadomian orogen preserved in the Elbe zone and the North Saxon antiform of the Saxo-Thuringian zone (NE Bohemian Massif) and from the Alcudian group of the Central Iberian zone in Iberia. Sedimentary and other features of the deposits further allow tracing a glacial event within sedimentary rocks related

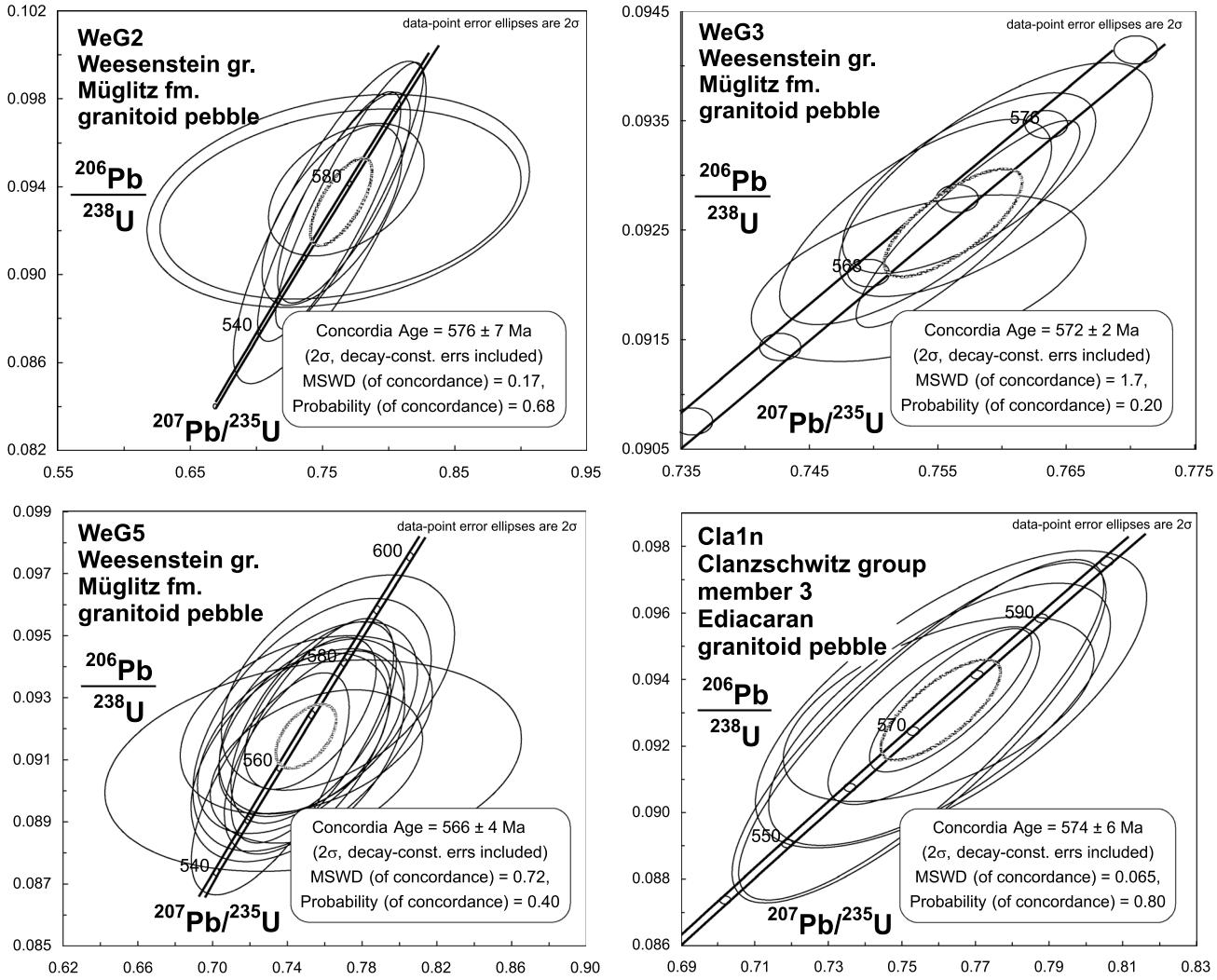


**Fig. 15** U–Pb LA–ICP–MS zircon ages of three granitoid pebbles from the Müglitz formation of the Weesenstein group (Weesenstein diamictite) and from one granitoid pebble from member 3 of the Clanzschwitz group (Clanzschwitz diamictite)

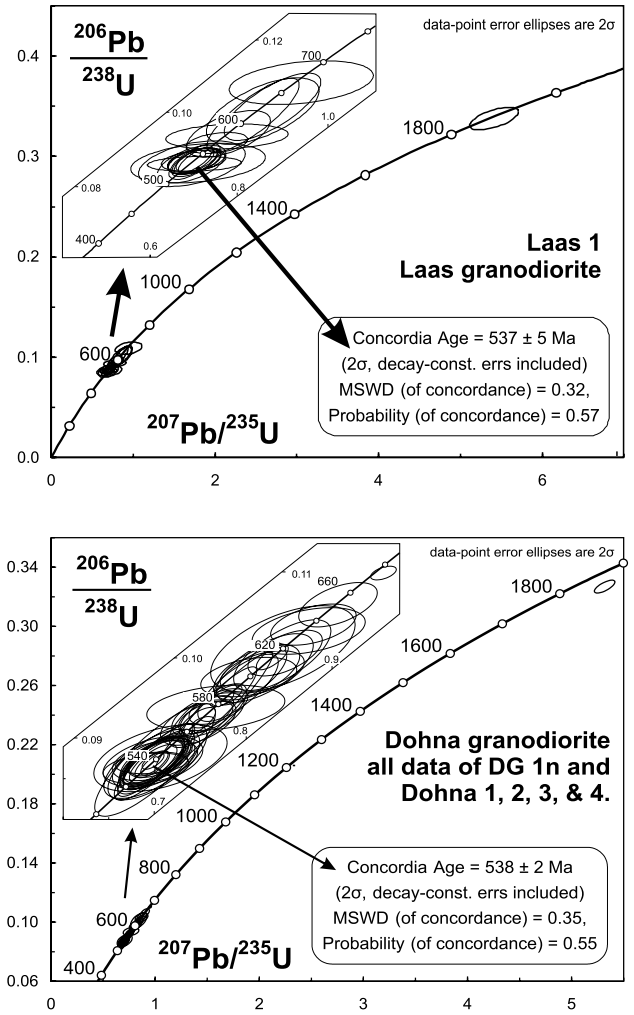


**Fig. 16** U-Pb ages from the granodiorites of Laas (*top*) and Dohna (*bottom*). For the Dohna granodiorite, U-Pb LA–ICP–MS zircon ages of five different samples were used (DG1n, Dohna 1–4). In the lower right diagram, a Concordia age of 538 ± 2 Ma is shown, which was calculated from the youngest zircon population of all samples. In addition, the diagram shows the large amount of inherited zircon grains occurring in the Dohna granodiorite

to the Cadomian orogen (Weesenstein and Clanzschwitz groups, and Lower Alcudian group). Indicative for glaciomarine deposition are dropstones, flatiron-shaped pebbles ("*Bügeleisen-Geschiebe*"), facetted pebbles, dreikanters, rainout sediments, and zircon grains affected by ice abrasion. Pre-glacial and glaciomarine sedimentation took place in a time span between c. 565 and 540 Ma. Age constraints completely rule out a correlation of this glacial event recorded in the Cadomian metasedimentary rocks of the Saxo-Thuringian and Central Iberian zones with the Gaskiers glaciation, which occurred around 579–581 Ma (Bowring et al. 2002; Thompson et al. 2014; Pu et al. 2016). Instead, a correlation with a glacial event recorded in Northwest Africa (Morocco) (Vernhet et al. 2012) and in Saudi Arabia (Vickers-Rich and Fedonkin 2007) is much more realistic and provides more information about the timing of this young Neoproterozoic glacial event. At Bou Azzer (Moroccan Anti-Atlas), Vernhet et al. (2012) describe glaciomarine structures (striated pavement on rhyolites) within the Ouarzazate group. The age of the latter is constrained by published U–Pb ages of the Ouarzazate group and can be placed in a time window between c. 570 and 562 Ma (Karaoui et al. 2015). In Saudi Arabia, another glaciomarine diamictite has been detected in Ediacaran sedimentary deposits of the Dhaiqa formation. An ash bed just below the diamictite provided a U–Pb age of 560 ± 4 Ma (Vickers-Rich and Fedonkin 2007). Furthermore, an Ediacaran glacial deposit (Moelv diamictite) crops out in Baltica (Bingen et al. 2005). However, available age data are not sufficient to constrain an age younger than the Gaskiers glaciation (Bingen et al. 2005). All in all, Ediacaran diamictites of the Saxo-Thuringian zone are bracketed in a time range of 565–540 Ma. We correlate glacial deposits of Bohemia and Iberia with the closer occurrences of glaciomarine diamictites in the Anti-Atlas (Bou Azzer) and in Saudi Arabia (Dhaiqa formation), which suggest a sedimentation age closer to 565 Ma for the Weesenstein, Clanzschwitz, and Orellana diamictites. Because of the clear post-Gaskiers age of all these glacial deposits, the data allow to define a new Ediacaran glacial event younger than the Gaskiers glaciation. Because of the main occurrences, we propose to name the glacial event at c. 565 as Weesenstein–Orellana glaciation (Fig. 18).

Existence of this Cadomian glaciation could be the reason for the negative excursion of the $\delta^{13}C$ curve (Shuram–Wonoka anomaly) (Fig. 18; Halverson et al. 2005). The origin of the Shuram–Wonoka anomaly is under discussion. Le Guerroue et al. (2006) concluded that the anomaly was not related to glaciation, since it lasted 50 Myr, and that it included the Gaskiers glaciation (i.e., it began before the Gaskiers). They also suggested that it did not end until 550 Ma, which suggests that it is not caused by glaciation. Halverson et al. (2005) suggest duration of the Shuram–Wonoka anomaly between c. 590 and c. 560 Ma. A shorter time interval (581 ± 6–567 ± 6 Ma) is inferred by an age model of Retallack et al. (2014). All in all, precise timing and the basic cause for the Shuram–Wonoka anomaly are not well known, but Ediacaran glaciations certainly contributed to that negative anomaly, because glacial events require a response in the ocean water chemistry.

Glacigenic sedimentary and related rocks act as an archive of evolution of the hinterland. The Hf isotope record of detrital and magmatic zircons from investigated strata gives some

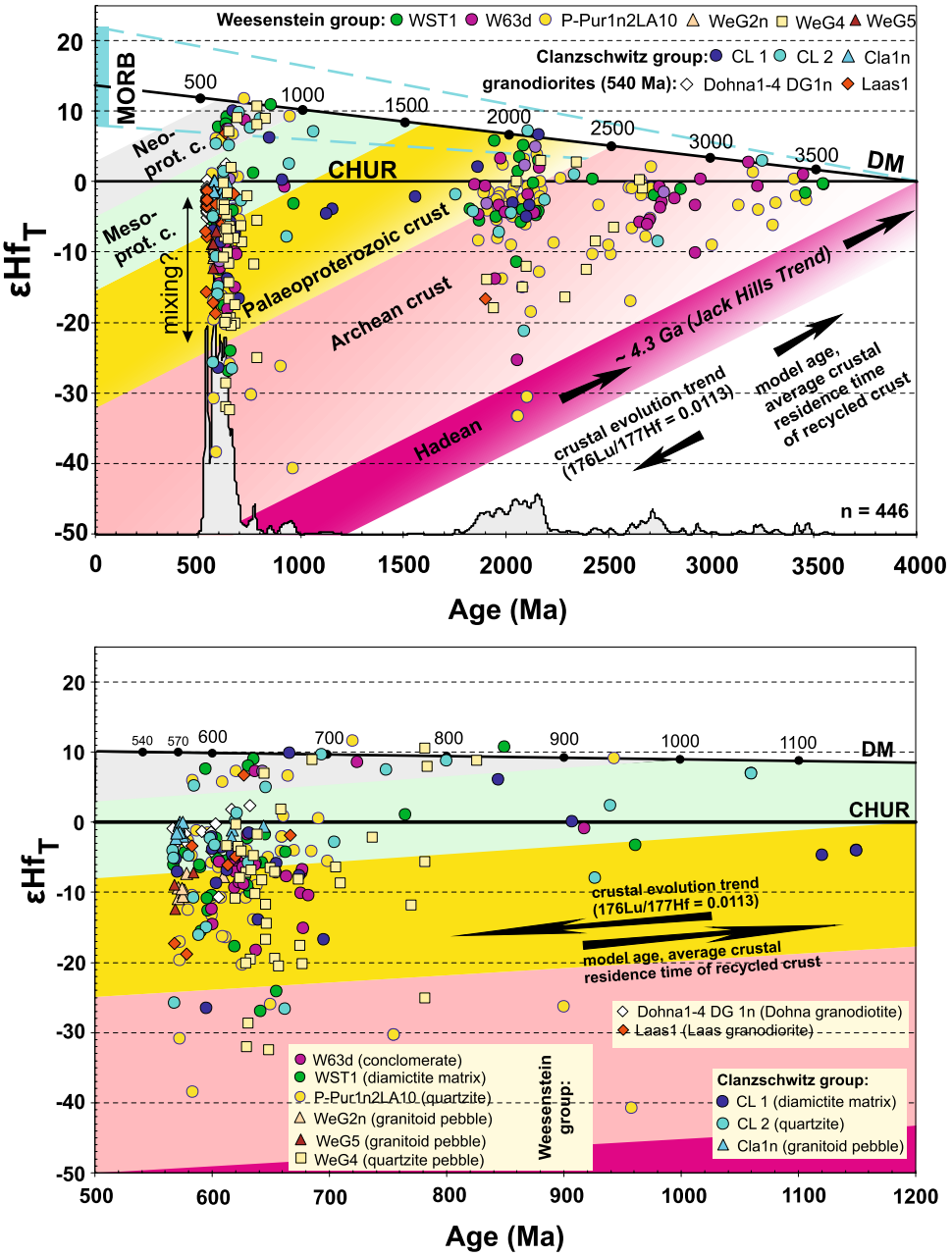


**Fig. 17** Hf isotope evolution diagrams summarizing the data of zircons from the studied metasedimentary rocks of the Weesenstein and Clanzschwitz groups. The probability plot of the zircon age populations is represented in *grey*. See text for discussion. *Top* Hf isotope evolution diagram of analyzed zircon grains in the age range of ca. 500–4000 Ma. *Below* Hf isotope evolution diagram of analyzed zircon grains in the age range of 500–1200 Ma. For details and references of depleted mantle evolution, see Gerdes and Zeh (2006) and Dhuime et al. (2011). Data were analyzed using the decay constant of $1.867 \times 10^{-11}$ (Scherer et al. 2001) and the CHUR parameters of Bouvier et al. (2008)

clues about the nature of the major geologic events forming the Cadomian orogen and its West African hinterland. The Cadomian crustal evolution is dominated by the recycling of continental crust as suggested by the dominance of zircons with negative $\varepsilon Hf_i$ values. Juvenile arc magmas became contaminated by the recycling of Eburnean and Archaean crust during long Cadomian magmatic arc activity. A minority of the zircons consists of those derived from the depleted mantle array. Mixture with continental crust is always present. The required geotectonic setting is a continental magmatic arc developed during the Neoproterozoic on stretched Archaean and Palaeoproterozoic (Eburnean) crust.

For the West African hinterland, important episodes of crustal growth and/or recycling can be defined: (1) a 2.2–4.3 Ga old basement became recycled in most cases during Eburnean (c. 1.8–2.2 Ga) orogenic processes; (2) two Eburnean zircons found in the Purpurberg quartzite member and aged at 2056 ± 34 and 2103 ± 40 Ma imply recycling of pre-existing Hadean crust and show $T_{DM}$ model ages of 4.21 and 4.27 Ga, respectively (Jack Hills trend). Hadean

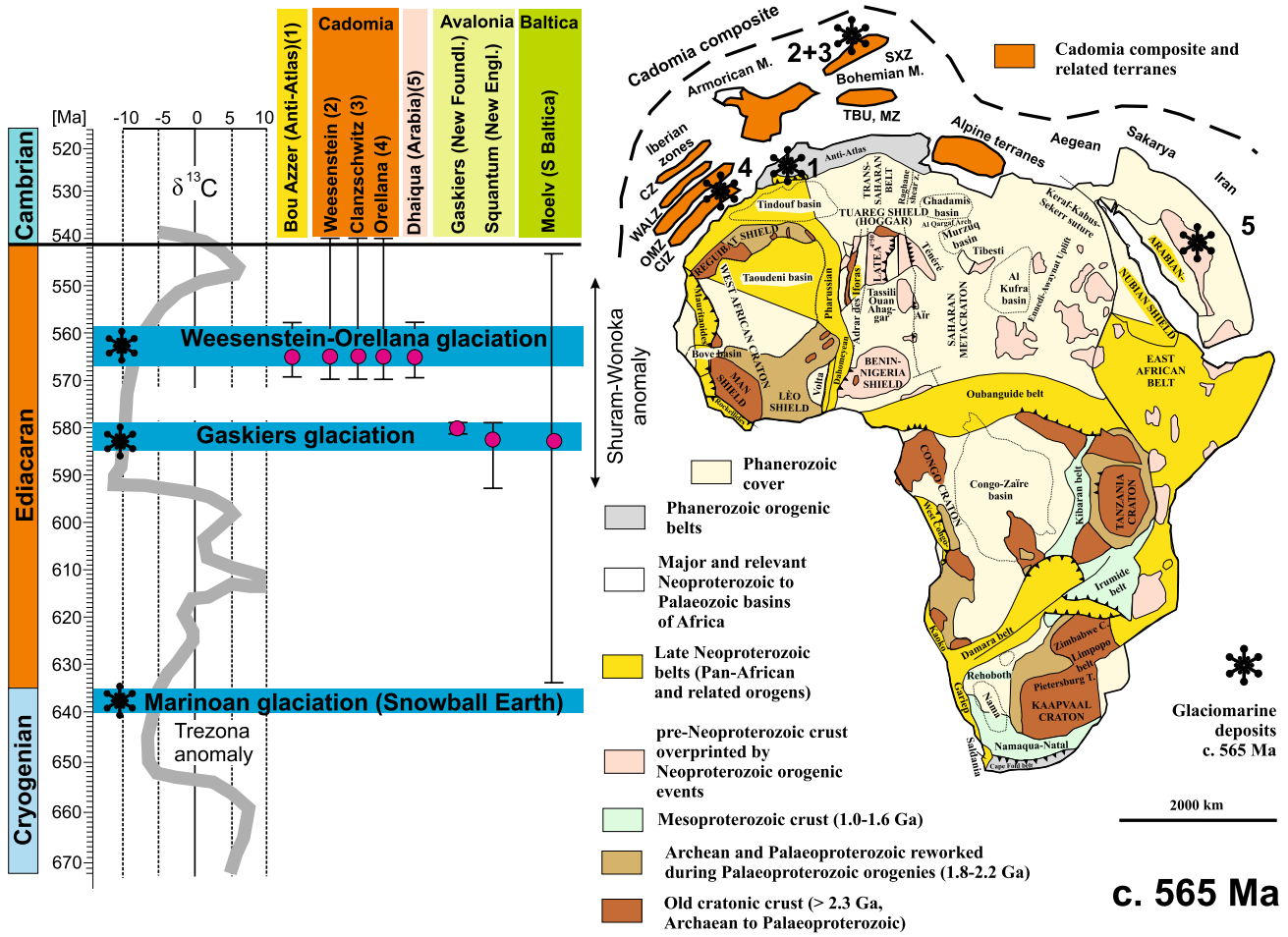


**Fig. 18** Timing of the Weesenstein–Orellana glaciation and its relation to the $\delta^{13}C$ curve (Halverson et al. 2005) (*left*); palinspastic map showing palaeopositions of Ediacaran post-Gaskiers glacial deposits in peri-Gondwana, North Africa, and Arabia (*right*). Cadomia composite includes the different terranes of the Cadomian orogen distributed now in Western and Central Europe (peri-Gondwanan West Africa)

crust existed until c. 2.0 Ga; (3) juvenile zircons are scarce; (4) Archean magmas recycled a c. 2.7–3.8 Ga old crust; and (5) zircons with ages of 3.2–3.3 and 3.4–3.5 Ga show a juvenile trend.

**Acknowledgements** This is a contribution to IGCP project 648 "Supercontinent Cycles and Global Geodynamics". Gregory J. Retallack (Eugene) and an unknown reviewer are thanked for their helpful reviews. We thank the Australian IGCP Committee for their funding support for the work in Saudi Arabia as well as the UNESCO IGCP Board for project IGCP587. Special thanks go to Fayek Kattan and his team from the Saudi Geological Survey for facilitating our work in Saudi Arabia.

## References

Abati J, Aghzer AM, Gerdes A, Ennih N (2010) Detrital zircon ages of Neoproterozoic sequences of the Moroccan anti-atlas belt. Precambr Res 181(1–4):115–128

Abati J, Aghzer AM, Gerdes A, Ennih N (2012) Insights on the crustal evolution of the West African Craton from Hf isotopes in detrital zircons from the Anti-Atlas belt. Precambr Res 212–213:263–274

Álvarez-Nava Oñate H, García Casquero JL, Gil Toja A, Hernández Urroz J, Lorenzo Álvarez S, López Díaz F, Mira López M, Monteserín López V, Nozal Martín F, Pardo Alonso MV, Picart Boira J, Robles Casas R, Santamaría Casanovas J, Solé FJ (1988) Unidades litoestratigráficas de los materiales Precámbrico-Cámbricos en la mitad suroriental de la zona Centro-Ibérica. II Congreso Geológico de España, Comunicaciones 1:19–22

Bao H, Lyons JR, Zhou C (2008) Triple oxygen isotope evidence for elevated $CO_2$ levels after a Neoproterozoic glaciation. Nature 453(7194):504–506

Bingen B, Griffin WL, Torsvik TH, Saeed A (2005) Timing of Late Neoproterozoic glaciation on Baltica constrained by detrital zircon geochronology in the Hedmark Group, south-east Norway. Terra Nova 17:250–258

Black R, Latouche L, Liégeois JP, Caby R, Bertrand JM (1994) Pan-African displaced terranes of the Tuareg Shield (central Sahara). Geology 22:641–644

Bouvier A, Vervoort JD, Patchet PJ (2008) The Lu-Hf and Sm-Nd isotopic composition of CHUR: constraints from unequilibrated chondrites and implications for the bulk composition of terrestrial planets. Earth Planet Sci Lett 273(1–2):48–57

Bowring SA, Landing E, Myrow P, Ramezani J (2002) Abstract #13045: geochronological constraints on terminal Neoproterozoic events and the rise of metazoans. Astrobiology 2:457–458

Chauvel C, Levin E, Carpentier M, Arndt NT, Marini JC (2008) Role of recycled oceanic basalt and sediment in generating the Hf-Nd mantle array. Nat Geosci 1:64–67

Clariana García MP, Rubio Pascual F, Montes Santiago MJ, González Clavijo EJ (2017) Continuous digital Geologic Map E1:50,000, Zona Centroibérica. Dominio esquisto-grauváquico y Cuenca del Guadiana (Zona-1400) in GEODE. Mapa Geológico Digital continuo de España (online). http://igme.maps.arcgis.com/home/webmap/viewer.html?webmap=44df600f5c6241b59edb596f54388ae4. Accessed 9 Aug 2017

Condon DJ, Bowring SA (2011) A user's guide to Neoproterozoic geochronology. Geol Soc Lond Mem 36(1):135–149

Dhuime B, Hawkesworth C, Cawood P (2011) When continents formed. Science 331:154–155

Drost K, Gerdes A, Jeffries T, Linnemann U, Storey C (2011) Provenance of Neoproterozoic and early siliciclastic rocks of the Teplá-Barrandian unit (Bohemian Massif): evidence from U-Pb detrital zircon ages. Gondwana Res 19:213–231

Fuenlabrada JM, Pieren AP, Díez Fernández R, Sánchez Martínez S, Arenas A (2016) Geochemistry of the Ediacaran–Early Cambrian transition in Central Iberia: tectonic setting and isotopic sources. Tectonophysics 681:15–30

García-Hidalgo JF, Pieren Pidal AP, Olivé Davó A, Carbajal Menéndez A, de la Fuente Krauss JV, Moreno F, Cantos Robles R, Liñán E (1993) Memoria de la Hoja 779 "Villanueva de La Serena". Mapa Geológico de España 1:50.000 (2ª Serie). IGME, Madrid

Gärtner A, Villeneuve M, Linnemann U, El Archi A, Bellon H (2013) An exotic terrane of Laurussian affinity in the Mauritanides and Souttoufides (Moroccan Sahara). Gondwana Res 24(2):687–699

Gehmlich M (2003) Die Cadomiden und Variszziden des Saxothuringischen Terranes—Geochronologie magmatischer Ereignisse. Freib Forsch C500:1–129

Gerdes A, Zeh A (2006) Combined U-Pb and Hf isotope LA-(MC-) ICP-MS analysis of detrital zircons: comparison with SHRIMP and new constraints for the provenance and age of an Armorican metasediment in Central Germany. Earth Planet Sci Lett 249:47–61

Gerdes A, Zeh A (2009) Zircon formation versus zircon alteration—new insights from combined U-Pb and Lu-Hf in situ LA-ICP-MS analyses, and consequences for the interpretation of Archean zircon from the Central Zone of the Limpopo Belt. Chem Geol 261(3–4):230–243

Graindor MJ (1957) Le Briovérian dans le Nord-East du massif Armoricain. Mém. Carte Géol. Dét., France, pp 1–111

Gutiérrez-Alonso G, Fernández-Suárez J, Jeffries TE, Jenner GA, Tubret MN, Cox R, Jackson SE (2003) Terrane accretion and dispersal in the northern Gondwana margin. An Early Palaeozoic analogue of a long-lived active margin. Tectonophysics 365:221–232

Halverson GP, Hoffman PF, Schrag DP, Maloof AC, Rice AHN (2005) Toward a Neoproterozoic composite carbon isotope record. GSA Bulletin 117:1181–1207

Hebert CL, Kaufman AJ, Penniston-Dorland SC, Martin AJ (2010) Radiometric and stratigraphic constraints on terminal Ediacaran (post-Gaskiers) glaciation and metazoan evolution. Precambr Res 182:402–414

Hoffman PF (2009) Pan-glacial—a third state in the climate system. Geol Today 25(3):100–107

Hoffman PF, Kaufman AJ, Halverson GP, Schrag DP (1998) A neoproterozoic snowball Earth. Sci N Ser 281(5381):1342–1346

Hoffmann KH, Condon DJ, Bowring SA, Crowley JL (2004) U-Pb zircon date from the Neoproterozoic Ghaub Formation Namibia: constraints on Marinoan glaciation. Geology 32(9):817–820

Hofmann M, Linnemann U, Gerdes A, Ullrich B, Schauer M (2009) Timing of dextral strike-slip processes and basement exhumation in the Elbe Zone (Saxo-Thuringian Zone): the final pulse of the Variscan Orogeny in the Bohemian Massif constrained by LA-SF-ICP-MS U–Pb zircon data. In: Murphy JB, Keppie JD, Hynes AJ (eds) Ancient orogens and modern analogues, vol 327. The Geological Society, London, pp 197–214

Horstwood MSA, Košler J, Gehrels G, Jackson SE, McLean NM, Paton C, Pearson NJ, Sircombe K, Sylvester P, Vermeesch P, Bowring JF, Condon DJ, Schoene B (2016) Community-derived standards for LA-ICP-MS U-Th-Pb geochronology—uncertainty propagation, age interpretation and data reporting. Geostand Geoanal Res 40:311–332

Immonen N (2013) Surface microtextures of ice-rafted quartz grains revealing glacial ice in the Cenozoic Arctic. Oalaeogeogr Palaeoclimatol Palaeoecol 374:293–302

Julivert M, Fontboté JM, Ribeiro A, Conde LS (1972/1974) Mapa Tectónico de la Península Ibérica y Baleares a escala 1:1.000.000 y Memoria Explicativa. IGME, Madrid

Karaoui B, Breitkreuz C, Mahmoudi A, Youbi N, Hofmann M, Gärtner A, Linnemann U (2015) U–Pb zircon ages from volcanic and sedimentary rocks of the Ediacaran Bas Draâ inlier (Anti-Atlas Morocco): chronostratigraphic and provenance implications. Precambr Res 263:43–58

Kirschvink JL (1992) Late Proterozoic low-latitude global glaciation: the Snowball Earth. In: Schopf JW, Klein C (eds) The Proterozoic Biosphere. A multidisciplinary study. Cambridge University Press, Cambridge, pp 51–52

Kirschvink JL, Gaidos EJ, Bertani LE, Beukes NJ, Gutzmer J, Maepa LN, Steinberger RE (2000) Paleoproterozoic snowball earth: extreme climatic and geochemical global change and its biological consequences. Proc Natl Acad Sci USA 97(4):1400–1405

Le Guerroue E, Allen PA, Cozzi A, Etienne JL, Fanning M (2006) 50 Myr recovery from the largest negative δ13C excursion in the Ediacaran Ocean. Terra Nova 18:147–153

Linnemann U (1990) Lithostratigraphische und sedimentologische Untersuchung präsudetischer Sedimentabfolgen der südlichen Elbezone unter besonderer Berücksichtigung der Weesensteiner Gruppe (Jungproterozoikum) und der Mühlbach/Häselich-Nossener Gruppe (Kambro-Ordovizium). PhD Thesis, Bergakademie Freiberg, pp 1–120

Linnemann U (1991) Glazioeustatisch kontrollierte Sedimentationsprozesse im Oberen Proterozoikum der Elbezone (Weesensteiner Gruppe/Sachsen). Zbl Geol Paläontol 12(1):2907–2934

Linnemann U (1994) Geologischer Bau und Strukturentwicklung der südlichen Elbezone. Abh. Staatl Mus Min Geol zu Dresden 40:7–36

Linnemann U (2007) Ediacaran rocks from the Cadomian basement of the Saxo-Thuringian Zone (NE Bohemian Massif, Germany): age constraints, geotectonic setting and basin development. In: Vickers-Rich P, Komarower P (eds) the rise and fall of the Ediacaran Biota, vol 286. The Geological Society, London, pp 35–51

Linnemann U, Gehmlich M, Tichomirowa M, Buschmann B, Nasdala L, Jonas P, Lützner H, Bombach K (2000) From Cadomian subduction to Early Paleozoic rifting: the evolution of Saxo-Thuringia at the margin of Gondwana in the light of single zircon geochronology and basin development (Central European Variscides, Germany). Geol Soc Lond Spec Publ 179:131–153

Linnemann U, Drost K, Gerdes A, Jeffries T, Romer RL (2008) The Bohemian Massif (Chapter 3: "The Cadomian Orogeny"). In:

McCann T (ed) The geology of Central Europe. The Geological Society of London, London, pp 121–147
Linnemann U, Romer RL, Gerdes A, Jeffries TE, Drost K, Ulrich J (2010a) The cadomian orogeny in the Saxo-Thuringian zone. In: Linnemann U, Romer RL (eds) Pre-mesozoic geology of Saxo-Thuringia—from the cadomian active margin to the Variscan orogen. Schweizerbart Science, Stuttgart, pp 37–58
Linnemann U, Hofmann M, Romer RL, Gerdes A (2010b) Transitional stages between the Cadomian and Variscan Orogenies: Basin development and tectonomagmatic evolution of the southern margin of the Rheic Ocean in the Saxo-Thuringian Zone (North Gondwana shelf). In: Linnemann U, Romer RL (eds) Pre-mesozoic geology of Saxo-Thuringia—from the cadomian active margin to the Variscan orogen. Schweizerbart Science, Stuttgart, pp 59–98
Linnemann U, Ouzegane K, Drareni A, Hofmann M, Becker S, Gärtner A, Sagawe A (2011) Sands of West Gondwana: an archive of secular magmatism and plate interactions—a case study from the Cambro-Ordovician section of the Tassili Ouan Ahaggar (Algerian Sahara) using U-Pb-LA-ICP-MS detrital zircon ages. Lithos 123(1–4):188–203
Linnemann U, Gerdes A, Hofmann M, Marko L (2014) The Cadomian Orogen: neoproterozoic to Early Cambrian crustal growth and orogenic zoning along the periphery of the West African Craton—Constraints from U–Pb zircon ages and Hf isotopes (Schwarzburg Antiform, Germany). Precambr Res 244:236–278
Lotze F (1945) Zur Gliederung des Varisciden der Iberischen Meseta. Geotekt Forsch 6:78–92
Ludwig KR (2001) Users Manual for Isoplot/Ex rev. 2.49: Berkeley Geochronology Center Special Publication No. 1a, pp 1–56
Macdonald FA, Schmitz MD, Crowley JL, Roots CF, Jones DS, Maloof AC, Strauss JV, Cohen PA, Johnston DT, Schrag DP (2010) Calibrating the cryogenian. Science 327(5970):1241–1243
Narbonne GM, Gehling JG (2003) Life after snowball: the oldest complex Ediacaran fossils. Geology 31(1):27–30
Narbonne GM, Xiao S, Shields G (2012) Ediacaran Period (Chapter 18) In: Gradstein FM, Ogg JG, Schmidt MD, Ogg GM (eds) Geologic Time Scale 2012. Elsevier, pp 427–449
Narbonne GM, Laflamme M, Trusler PW, Dalrymple RW, Greentree C (2014) Deep-water Ediacaran fossils from northwestern Canada: taphonomy, ecology, and evolution. J Paleontol 86:207–223
Ogg JG, Ogg GM, Gradstein FM (2016) A concise geologic time scale. Elsevier, pp 1–234
Ovtracht A, Tamain G (1970) Essai tectonique en Sierra Morena (Espagne). Congrès national des sociétés savantes. Sciences, Reims. C 95 T1, pp 305–327
Pieren AP (2000) Las sucesiones anteordovícicas de la región oriental de la provincia de Badajoz y área contigua de la de Ciudad Real. PhD Thesis, Universidad Complutense Madrid, pp 1–620
Pietzsch K (1917) Das Elbtalschiefergebiet südwestlich von Pirna. Zeitschrift der Deutschen Geologischen Gesellschaft 69:178–286
Pietzsch K (1927) Der Bau des erzgebirgisch-lausitzer Grenzgebietes. Abhandlungen des Sächsischen Geologischen Landesamts 2:1–28
Pietzsch K (1962) Geologie von Sachsen. VEB Deutscher Verlag der Wissenschaften Berlin, pp 1–870
Potrel A, Peucat JJ, Fanning CM, Auvray B, Burg J-P, Caruba C (1996) 3.5 Ga old terranes in the West African Craton, Mauritania. J Geol Soc 153(4):507–510
Potrel A, Peucat JJ, Fanning CM (1998) Archean crustal evolution of the West African Craton: example of the Amsaga Area (Reguibat Rise) U–Pb and Sm–Nd evidence for crustal growth and recycling. Precambr Res 90:107–117
Prave AR, Condon DJ, Hoffmann KH, Tapster S, Fallick AE (2016) Duration and nature of the end-Cryogenian (Marinoan) glaciation. Geology 44(8):631–634
Pu JP, Bowring SA, Ramezani J, Myrow P, Raub TD, Landing E, Mills A, Hodgin E, Macdonald FA (2016) Dodging snowballs: geochronology of the Gaskiers glaciation and the first appearance of the Ediacaran biota. Geology 44(11):955–958
Quesada C (1990) Precambrian successions in SW Iberia: their relationship to ´Cadomian´ orogenic events. In: D´Lemos RS, STrachan, RA, Topley, CG (eds) The Cadomian orogeny, vol 51. The Geological Society, London, pp 353–362
Quesada C (1991) Geological constraints on the Paleozoic tectonic evolution of tectonostratigraphic terranes in the Iberian Massif. Tectonophysics 185:225–245
Quesada C (1996) Evolución geodinámica de la zona Ossa-Morena durante el ciclo Cadomiense. In: Livro de Homenagem aõ Prof. Francisco Gonçalves, Uniniversidade de Évora, pp 205–230
Quesada C (2006) The Ossa-Morena Zone of the Iberian Massif: a tectonostratigraphic approach to its evolution. Z Dtsch Ges Geowiss 157(4):585–595
Retallack GJ, Marconato A, Osterhout JT, Watts KE, Bindeman IN (2014) Revised Wonoka isotopic anomaly in South Australia and Late Ediacaran mass extinction. J Geol Soc 171:709–722
Rocci G, Bronner G, Deschamps M (1991) Crystalline basement of the West African Craton. The West African Orogens and Circum-Atlantic Correlatives. Springer, Berlin, pp 31–61
Rooney AD, Strauss JV, Brandon AD, Macdonald FA (2015) A Cryogenian chronology: two long-lasting synchronous neoproterozoic glaciations. Geology 43(5):459–462
San José MA, Pieren Pidal AP, García-Hidalgo JF, Vilas Minondo L, Herranz Araújo P, Peláez Pruneda JR, Perejón A (1990) Ante-Ordovician stratigraphy. In: Dallmeyer RD, Martínez García E (eds) Premesozoic geology of Iberia. Springer, pp 147–159
Sánchez-García T, Bellido F, Quesada C (2003) Geodynamic setting and geochemical signatures of Cambrian-Ordovician rift-related igneous rocks (Ossa-Morena Zone, SW Iberia). Tectonophysics 365:233–255
Sánchez-García T, Quesada C, Bellido F, Dunning G, González de Tánago J (2008) Two-step magma flooding of the upper crust during rifting: the Early Paleozoic of the Ossa-Morena Zone (SW Iberia). Tectonophysics 461:72–90
Sánchez-García T, Bellido F, Pereira MF, Chichorro M, Quesada C, Pin C, Silva JB (2010) Rift-related volcanism predating the birth of the Rheic Ocean (Ossa-Morena zone, SW Iberia). Gondwana Res 17:392–407
Scherer E, Münker C, Mezger K (2001) Calibration of the Lutetium-Hafnium clock. Science 293:683–687
Schmidt K (1960) Die Geröllführung algonkisch-kambrischer Grauwacken des Westlausitzer Zuges. Freiberger Forschungsheft C 91:1–79
Sebastian U (2013) Die Geologie des Erzgebirges. Springer, pp 1–268
Sircombe KN (2004) AGE DISPLAY: an EXCEL workbook to evaluate and display univariate geochronological data using binned frequency histograms and probability density distributions. Comput Geosci 30:21–31
Sláma J, Košler J, Condon DJ, Crowley JL, Gerdes A, Hanchar JM, Horstwood MSA, Morris GA, Nasdala L, Norberg N, Schaltegger U, Schoene B, Tubret MN, Whitehouse MJ (2008) Plešovice zircon-a new natural reference material for U-Pb and Hf isotopic microanalysis. Chem Geol 249:1–35
Stacey JS, Kramers JD (1975) Approximation of terrestrial lead isotope evolution by a two-stage model. Earth Planet Sci Lett 26:207–221
Talavera C, Martínez Poyatos D, González Lodeiro F (2015) SHRIMP U-Pb geochronological constraints on the timing of the intra-Alcudian (Cadomian) angular unconformity in the Central Iberian Zone (Iberian Massif, Spain). Int J Earth Sci 104:1739–1757
Thompson MD, Ramezani J, Crowley JL (2014) U-pb zircon geochronology of roxbury conglomerate, boston basin, massachusetts: tectonostratigraphic implications for avalonia in and beyond SE New England. Am J Sci 314(6):1009–1040
Vernhet E, Youbi N, Chellai EH, Villeneuve M, El Archi A (2012) The Bou-Azzer glaciation: evidence for an Ediacaran glaciation on

the West African Craton (Anti-Atlas, Morocco). Precambr Res 196–197:106–112

Vickers-Rich P, Fedonkin MA (2007) The proterozoic (2.5 billion to 542 million years ago). In: Fedonkin MA, Gehling JG, Grey K, Narbonne GM, Vickers-Rich P (eds) The rise of animals. The Johns Hopkins University Press, Baltimore, pp 29–51

Wilde SA, Valley JW, Peck WH, Graham CM (2001) Evidence from detrital zircons for the existence of continental crust and oceans on the Earth 4.4 Gyr ago. Nature 409:175–178

Zieger J (2015) U–Pb-Datierung an magmatischen und detritischen Zirkonen des Döhlener Beckens. Master Thesis, Technische Universität Dresden, pp 1–141